Genomic surveillance for multidrug-resistant or hypervirulent *Klebsiella pneumoniae* among bloodstream isolates at a United States academic medical center

Travis J. Kochan[1], Sophia H. Nozick[1], Rachel L. Medernach[1,2], Bettina H. Cheung[1], Samuel W.M. Gatesy[2], Marine Lebrun-Corbin[1], Sumitra D. Mitra[1], Natalia Khalatyan[1], Fiorella Krapp[2], Chao Qi[3], Egon A. Ozer[2,4], Alan R. Hauser[1,2]

[1]Department of Microbiology-Immunology, Northwestern University, Feinberg School of Medicine, Chicago, IL, USA

[2]Division of Infectious Diseases, Department of Medicine, Northwestern University, Feinberg School of Medicine, Chicago, IL, USA

[3]Department of Pathology, Northwestern University, Feinberg School of Medicine, Chicago, Illinois, USA

[4]Center for Pathogen Genomics and Microbial Evolution, Havey Institute for Global Health, Northwestern University Feinberg School of Medicine, Chicago, IL, USA

Abstract

Background: *Klebsiella pneumoniae (K. pneumoniae)* strains have been divided into two major categories: classical *K. pneumonia,* which are frequently multidrug-resistant and cause hospital-acquired infections in patients with impaired defenses, and hypervirulent *K. pneumoniae,* which cause severe disseminated community-acquired infections in immunologically normal hosts. Both types of infections may lead to bacteremia and are associated with significant morbidity and mortality. The relative burden of these two types of *K. pneumoniae* among bloodstream isolates within the United States is not well understood.

Methods: We examined consecutive *K. pneumoniae* isolates cultured from the blood of hospitalized patients at Northwestern Memorial Hospital (NMH) in Chicago, Illinois April 2015 – April 2017. Bloodstream isolates underwent whole genome sequencing, and clinically relevant data (sequence type [ST], capsule loci, virulence factors, and antimicrobial resistance genes) were inferred from the genome using the bioinformatic tools *Kleborate* and *Kaptive.* Patient demographic, comorbidity, and infection information, as well as phenotypic antimicrobial resistance of the isolate were extracted from the electronic medical record. Candidate hypervirulent isolates were tested in a murine model of pneumonia. Complete genome sequences of these candidate hypervirulent isolates were obtained and plasmid content was evaluated.

Results: *K. pneumoniae* bloodstream isolates (n=104) from NMH were highly diverse consisting of 75 distinct STs and 51 unique capsule loci. The majority of these isolates (n=58, 55.8%) were susceptible to all tested antibiotics except ampicillin, but 17 (16.3%) were multidrug-resistant. A total of 32 (30.8%) of these isolates were STs of known high-risk clones, including ST258 and ST45. In particular, 18 (17.3%) were

resistant to ceftriaxone, 17 harbored extended-spectrum beta-lactamases, and 9 (8.7%) were resistant to meropenem. Four (3.8%) of the 104 isolates were hypervirulent *K. pneumoniae,* as evidenced by hypermucoviscous phenotypes, high levels of virulence in a murine model of pneumonia, and the presence of large plasmids similar to characterized hypervirulence plasmids. Of particular concern, several of these plasmids contained *tra* conjugation loci suggesting the potential for transmission. Two of these hypervirulent strains belonged to the well characterized ST23 lineage and one to the emerging ST66 lineage.

Conclusions: While NMH *K. pneumoniae* bloodstream infections are caused by highly diverse strains, the most prevalent STs were those of multidrug-resistant high-risk clones. A small number of hypervirulent *K. pneumoniae* were observed in patients with no recent travel history, suggesting that these isolates are undergoing community spread in the United States.

Introduction

Klebsiella pneumoniae (*K. pneumoniae*) is a leading cause of nosocomial infections worldwide including pneumonia, bloodstream, and urinary tract infections (1). This bacterium causes severe secondary pneumonia in patients with respiratory virus infections and is a leading cause of secondary pneumonia in patients with COVID-19 (2). *K. pneumoniae* pathogenicity is due to a variety of virulence factors, including siderophores, fimbriae, and polysaccharide capsules of various types. The polysaccharide capsule allows this bacterium to evade host immune defenses, such as complement-mediated phagocytosis (3, 4).

Most *K. pneumoniae* are referred to as “classical” (cKP), which infect chronically ill patients residing in hospitals and long-term care facilities (5). Some cKP strains have

become increasingly resistant to antibiotics, including carbapenems (6-11). A subgroup of cKP have been designated “high-risk clones,” lineages that are frequently multidrug-resistant (MDR) and extensively drug-resistant (XDR) and that have spread across continents to cause large numbers of infections (12). Some of the best characterized *K. pneumoniae* high-risk clones include ST11, ST14, ST15, ST17, ST147, ST258, ST307, and ST512. Within the United States, ST258 and ST307 are endemic high-risk clones that are carbapenem-resistant (CRE) and extended-spectrum-beta-lactamase-resistant (ESBL), respectively. Genes conferring antimicrobial resistance in these strains are often carried by conjugative plasmids that allow for dissemination among cKP strains. Thus, it is not surprising that the IDSA, WHO, and the CDC have each deemed MDR *K. pneumoniae* as a serious public health priority in need of new therapeutic development (13-15).

A second type of *K. pneumoniae*, referred to as hypervirulent *K. pneumoniae* (hvKP), was first identified in Taiwan in 1986 as a common cause of pyogenic liver abscesses (PLA) in young, otherwise healthy individuals living in the community (16-23). Other than diabetes mellitus, these patients lacked risk factors commonly associated with cKP infections. While these strains are now common in Asia, little is known about their prevalence in the United States. Case reports document the presence of hvKP infections in North America, but only a few surveillance studies have been performed (22, 24-26). hvKP strains frequently express highly mucoid capsules, leading to a “hypermucoviscous” (hmv) colony phenotype, and are considerably more virulent in mouse models than cKP strains (27). Their increased virulence is usually attributed to the presence of one of several large, non-conjugative “hypervirulence” plasmids (28-30). The non-conjugative nature of these plasmids and the limitations imposed by the hyper-mucoid capsule on genetic exchange may restrict the hypervirulence phenotype to

strains of a few sequence types (e.g. ST23, ST86, ST66) and capsule loci (e.g. KL1, KL2)(18, 31, 32). Detection of hvKP is clinically important, as they may cause infections that require prolonged antibiotic therapy, that tend to relapse, and that frequently disseminate to remote sites (33).

Hypervirulence plasmids are defined by several pathogenic features. In general, these plasmids contain two distinct pathogenicity loci (PAL-1 and PAL-2) (Fig 1A). PAL-1 usually consists of a mucoid regulator gene (*rmpA2*), the aerobactin receptor gene (*iutA*), and aerobactin biosynthesis genes (*iucABCD*). PAL-2 usually consists of a distinct mucoid regulator operon (*rmpADC*), the salmochelin receptor gene (*iroN*), and salmochelin biosynthesis genes (*iroBD*) (Fig 1A). However, considerable diversity exists among individual hypervirulence plasmids (30, 34). For example, pK2044 and KP52.145pII, two of the most common and best characterized hypervirulence plasmids, differ in that KP52.145pII contains an incomplete PAL-1 that lacks *rmpA2* (Fig 1A, B, C). We previously identified plasmid pTK421_2 from a *K. pneumoniae* bloodstream isolate from Northwestern Memorial Hospital (NMH) in Chicago, Illinois (Fig 1D) (35). This plasmid also lacks *rmpA2* but contains conjugation genes (Fig 1D). The population diversity of hypervirulence plasmids remains poorly defined but is an area of active investigation.

The hypervirulence plasmids contribute to the pathogenicity of hvKP strains in several ways. The mucoid regulators *rmpA* and *rmpA2* increase capsule production and hypermucoviscosity (29), and the siderophores are thought to provide access to host-sequestered iron reserves. However, the relative roles of the different accessory siderophores (aerobactin, salmochelin, and yersiniabactin) in hvKP virulence remain controversial (36, 37). A 2015 report suggested that aerobactin was the only siderophore required for the hypervirulence phenotype of the ST86-K2 capsule type strain hvKP1 in

both mouse intraperitoneal and pneumonia models (37). In contrast, another report showed that only a triple siderophore mutant (yersiniabactin, aerobactin, and salmochelin) of the ST23-K1 strain NTUH-K2044 was attenuated in the mouse intraperitoneal model (36). In addition, strain ATCC43816 (also called KPPR1) is hypervirulent in a mouse model of pneumonia but is otherwise atypical in that it lacks a hypervirulence plasmid and PAL-1 but contains a chromosomal version of PAL-2 in an integrative and conjugative element (ICEKp1, Fig 1A) (4, 38). In KPPR1, yersiniabactin promoted disease in the lung and salmochelin promoted dissemination to tissues (39). Thus, it is clear that mucoid regulators and siderophores play roles in conferring the hypervirulent phenotype, but significant strain-to-strain variability may occur.

As mentioned, hvKP strains were first identified based upon the unusual disease manifestations they cause (e.g. PLA), but considerable effort has been devoted to developing a microbiological definition that could be used by clinical laboratories to identify these strains. There are three characteristics commonly associated with hvKP: 1) hypermucoid capsules, 2) presence of hvKP pathogenicity loci, and 3) high levels of virulence in mouse models of infection (5, 16, 18, 27, 31, 33, 40-45). Initially, hypermucoviscosity was used as a proxy for the hvKP phenotype. However, several reports have described hmv *K. pneumoniae* strains that lack pathogenicity loci usually associated with hvKP and are not hypervirulent in mice (46-48). As a result, genetic biomarkers have been used to define hvKP, but these definitions have varied from study to study. Recently, Russo and colleagues systematically examined the accuracy of using *rmpA*, *rmpA2*, *peg-344*, *iucA*, and *iroB*, as diagnostic biomarkers for hvKP (27, 49). In their cohort of 175 isolates, the presence of *iucA*, *iroB* or a hmv phenotype distinguished hvKP from cKP with an accuracy of 96%, 97%, and 90%, respectively.

We characterized 140 consecutive bloodstream isolates of *Klebsiella* from patients at NMH in Chicago, Illinois from 2015 – 2017. We sequenced and determined virulence gene content, antimicrobial resistant gene content, and hypermucoviscosity of these isolates. We identified numerous MDR cKP high-risk clones and several isolates that contained genomic, clinical, and virulence properties consistent with hvKP.

Results

Microbiological characteristics of *Klebsiella* bloodstream isolates

We collected 140 consecutive *Klebsiella spp.* isolates from 119 patients with positive blood cultures from 2015–2017 at NMH. The Clinical Microbiology Laboratory at NMH identified these isolates as *K. pneumoniae*. Note that the *Klebsiella pneumoniae* species complex has recently been subdivided into *Klebsiella variicola, Klebsiella quasipneumoniae subsp. quasipneumoniae*, *Klebsiella quasipneumoniae subsp. Similipneumoniae* (50). Thus, we performed Illumina whole genome sequencing of these presumptive *K. pneumoniae* bacteremia isolates to more definitively define their species. Among these isolates, 85% (n=119) were confirmed by whole-genome sequencing to be *K. pneumoniae* with the remaining isolates being *K. variicola* (n=16), *K. quasipneumoniae subsp. quasipneumoniae* (n=1), *K. quasipneumoniae subsp. similipneumoniae* (n=3), and *K. oxytoca* (n=1) (Fig S1). The 119 *K. pneumoniae* isolates were cultured from 101 patients and were highly diverse and consisted of 75 unique sequence types (STs) (Simpson's diversity index = 0.98), 51 unique capsule loci (KL) (Simpson's diversity index = 0.97), and 10 distinct O antigen serotypes (Simpson's diversity index = 0.69). After removing isolates of the same strain cultured repeatedly from the same patient, we determined that 104 *K. pneumoniae* strains were obtained from 101 patients. Three patients had two separate *K. pneumoniae* bloodstream

infections caused by distinct strains, which were included in this study. This collection includes several STs associated with carbapenem resistant high-risk clones such as ST258 (n=6), ST45 (n=6), ST29 (n=5), ST14 (n=3), ST17 (n=3), ST15 (n=3), ST147 (n=3). Two isolates belonged to the ESBL-containing high risk clone ST307 (Fig 2 & S2A). In addition, we identified three STs associated with hvKP: ST23 (n=2), ST66 (n=1), and ST380 (n=1) (Fig 2 & S2A). The most common KL-types were KL2 (n=7), KL107 (n=7), KL30 (n=6), KL25 (n=5), KL24 (n=4), KL28 (n=4), KL22 (n=4), and KL54 (n=4) (Fig S1B). The most common O antigen serotypes were O1 (n=38), O2 (n=27), and O3b (n=21) (Fig S2C). These findings indicate that bloodstream isolates at NMH are highly diverse with respect to their STs, capsule types, and O-antigen serotypes.

Antimicrobial Resistance Determinants

While many cKP are MDR, hvKP isolates tend to be susceptible to antibiotics. We therefore examined the antibiotic resistance profiles of the isolates in our collection. Since *K. pneumoniae* is inherently resistant to ampicillin, it was not surprising that 100% of the bloodstream isolates had MICs above the resistance threshold (Fig 2 & S3). Thirty-nine isolates (37.5%) were non-susceptible (29 resistant, 10 intermediate) to ampicillin/sulbactam, 17 (16.3%) were resistant to aztreonam, 23 (22.1%) were non-susceptible (21 resistant and one intermediate) to cefazolin, 18 isolates (17.3%) were resistant to ceftriaxone, 17 isolates (16.3%) were resistant to cefepime, and nine isolates (8.7%) were resistant to meropenem (Table S1, Fig 2 and S3). Among NMH 104 bloodstream isolates, 42% contained at least one acquired antimicrobial resistance gene (Table S1). Twelve isolates (11.5%) contained extended spectrum beta-lactamase genes and nine (8.7%) contained a carbapenamase gene (8 bla_{KPC-3}, 1 bla_{NDM-1}) (Fig

S4). *bla*$_{NDM-1}$ was found in an ST147 isolate, while *bla*$_{KPC-3}$ carbapenemase genes were found in ST258 (n=5), ST15 (n=2), and ST45 (n=1) strains (Table S1). One ST258 isolate, KPN88, did not contain a carbapenamase gene and was sensitive to several beta-lactams (Table S1 and Fig 2). The most common ESBL genes were *bla*$_{CTX-M-15}$ (n=7, 6.7%) and *bla*$_{SHV-12}$ (n=4, 3.8%) (Table S1 and Fig S4). Strains carrying *bla*$_{CTX-M-15}$ were highly drug resistant including all beta-lactams tested except meropenem (Fig S4A-F). Strains carrying *bla*$_{SHV-12}$ also carried genes predicted to confer carbapenem resistance (Fig 2 & S4A-F). Isolates containing carbapenamases and/or ESBLs also carried genes predicted to confer resistance to aminoglycosides, trimethoprim, sulfonamides, tetracycline, fluoroquinolones, and phenicols suggesting these strains contain one or more antimicrobial resistance plasmids (Table S1). The correlations between phenotypic beta-lactam resistance and the presence of beta-lactam genes was very strong. All isolates containing a carbapenemase gene were resistant to ampicillin/sulbactam, aztreonam, cefazolin, cefepime, ceftriaxone, and meropenem (Table S1). Nearly all Isolates predicted to produce an ESBL were non-susceptible to ampicillin/sulbactam (100%), aztreonam (94%), cefazolin (100%), cefepime (94%), ceftriaxone (100%) (Table S1). Only one isolate, KPN103, had considerable beta-lactam resistance but lacked an ESBL gene; however, this isolate did contain the gene encoding the non-ESBL beta-lactamase, *bla*$_{TEM-1D}$ (Table S1).

Of the 104 *K. pneumoniae* isolates, 34 (32.6%) were non-susceptible to the combination of trimethoprim and sulfamethoxazole (TMP/SMX) (Fig S3). Of these isolates 31 (29.8%) contained both the *dfrA* and *sul1/2/3* genes, which encode resistance to TMP/SMX. (Table S1). Two resistant isolates contained only *dfrA* and one contained only *sul2* (Table S1).

Eighteen isolates (17.3%) were resistant to ciprofloxacin (Fig S3). Each of these isolates contained either *qnrB* gene, or *a* mutation in the *gyrA* gene (Table S1).

Within the collection, non-susceptibility rates to tobramycin, gentamicin, and amikacin were 17.3%, 10.5%, and 1.9%, respectively (Fig S3). The overall prevalence of aminoglycoside modifying enzymes (AMEs) was 31.7% (n=33) (Table S1). The most common AMEs were streptomycin resistance genes *strA* and *strB* (n=22) and the streptomycin/spectinomycin adenyltransferase *aadA2* (n=10); however, isolates containing only these AMEs were sensitive to tobramycin, gentamicin, and amikacin (Table S1). The acetyltransferases *aac(6')-Ib-cr.V2* (n=7), *aac(3)-IId* (n=2), and *aac(3)-IIa* (n=2), and the phosphotransferases *aph(3)-Ia.v1 (n=5) and aph(3')-Ia (n=2)* were associated with nonsusceptibility to gentamicin and tobramycin (Table S1).

Collectively, 17 (16.3%) of the 104 isolates were MDR including 12 (11.5%) that were extensively drug-resistant (XDR) (Fig 2). These findings indicate the MDR bacteria comprise a substantial proportion of *K. pneumoniae* causing bloodstream infections at NMH and suggest that many strains carry mobile elements with multiple resistance genes.

Virulence Determinants

We next searched the *Klebsiella* genomes for genes associated with enhanced virulence. The siderophore yersiniabactin promotes pulmonary infections in animal models, is associated with more severe disease in human infections, and is produced by hvKP strains (4, 39, 51, 52). We identified yersiniabactin biosynthesis loci (*ybt*) in 37.5% (n=39) of 104 NMH bloodstream isolates (Fig 2 & Table 2). Eleven unique alleles of *ybt* were detected, the most common being *ybt* 10 (n=12), *ybt* 17 (n=11) and plasmid-borne *ybt* 4 (n=4) (Table S1). *ybt* and the colibactin biosynthesis locus, *clb*, are commonly

found together on an integrative conjugative element, *ICEKp10* (18). We identified 12 (11.5%) isolates that contained *ICEKp10* representing five STs (ST258, ST29, ST66, ST15, and ST240) (Table S1). Although *ICEKp10* is a marker for the globally distributed CG23-I sub-lineage, within the United States, *ICEKp10* is a strong marker for the epidemic ST258 lineage (18, 53).

In addition to *ybt* and *clb*, we screened our collection for the following previously published diagnostic biomarkers of hvKP: *iucA, iroB, rmpA, rmpA2,* and the hmv phenotype. *iucA* was identified in 5 (4.8%), *iroB* in 4 (3.8%), *rmpA* in 4 (3.8%), and *rmpA2* in 2 (1.9%) (Fig 2 & Table 2). These virulence genes tended to be clustered within the same few strains. Four isolates contained *iucA, iroB,* and *rmpA* (Table 1). Two of these four (KPN8 and KPN115) were ST23, a sequence type commonly associated with hvKP, and the other two (KPN49 and KPN165) were ST66 and ST380, respectively. A single isolate, KPN23, was ST881 and contained *iucA* but not *iroB* or *rmpA*. (Fig 2 & Table 2). Three distinct *iucA* alleles were identified: *iuc*1 (n=2, ST23), *iuc2* (n=2, ST66 & ST380), and *iuc3* (n=1, ST881) (Table 1). Although two strains contained the *rmpA2* gene, both had a frameshift mutation in a previously published homopolymer region of *rmpA2* (54). All *iuc*+ isolates were sensitive to every antibiotic tested, except ampicillin (Table S1). The collection was screened for hmv capsules by both string test and centrifugation. A total of 10 (9.6%) and 18 (17.3%) isolates, respectively, were positive for hypermucoviscosity by these two tests (Table 2), including all four of the isolates containing *iucA, iroB,* and *rmpA* but not the isolate containing only *iucA* (Table 1, Table S1). These data confirm previous reports that the string test is less sensitive than centrifugation for measuring hypermucoviscosity (48, 55). However, all *rmpA*+ isolates were positive by both string and centrifugation tests (Table S1). In addition, isolates were tested for tellurite resistance, a phenotype commonly encoded by pK2044 plasmids (Fig

1). Five isolates (4.8%) grew on tellurite, including the two hmv ST23 isolates that were positive for *rmpA, rmpA2*, *iro1* and *iuc1 alleles* (Table 2). These results suggested that these two isolates contained pK2044-like plasmids, while the two isolates containing *iro2, iuc2* and *rmpA* contained KP52.145pII-like plasmids. Collectively, these findings indicate that clinical isolates with genomic features of hvKP are circulating at NMH.

Analysis of Plasmid Content

Next, we sought to characterize the plasmids harbored by the five isolates containing salmochelin and/or aerobactin biosynthesis genes. To define plasmids sequences, we performed Nanopore long read sequencing on these isolates. Hybrid assembly with the Illumina short reads of the genomes revealed that each of these isolates harbored a large plasmid with some hvKP pathogenicity loci (Table 1). Two isolates (KPN8 and KPN115) contained plasmids with near complete alignment with pK2044, including plasmid replicons, *repB* and *IncHI1B* and pathogenicity loci, PAL-1 and PAL-2 (Fig 3 and Table 1). KPN165 harbored an *IncFIB(K)* plasmid with close alignments with KP52.145pII but not pK2044 (Fig 4A and S5). Similar to KP52.145pII, this plasmid contained a version of PAL-1 with *iucABCD* and *iutA* but lacking *rmpA2* (Fig 1 and 4A). Interestingly, KPN49 contained two plasmids: one (pKPN49_1) with an *IncFIB(K)* replicon and homology to KP52.145pII and a second (pKPN49_2) with an *IncFIA(HI1)* replicon and homology to KP52.145pI (Fig 4A and Table 1). However, the KP52.145pII-like plasmids of KPN49 and KPN165 were ~40 kB larger than KP52.145pII. Analysis of this 40 kB sequence revealed that it contained a *tra* conjugation locus with high sequence homology with KP52.145pI, a second plasmid contained by reference hvKP strain KP52.145 (Fig 4B) (34, 56). We also identified a similar chimeric

hypervirulence plasmid (99.0% identity) in a previously published ST380 strain, hvKP4 (Fig 4B) (57, 58). The fifth isolate, KPN23, carried on a two-replicon plasmid (*IncFIB(K)* and *IncFII(pKP91)*) with aerobactin biosynthetic genes and putative conjugative genes. This plasmid did not resemble known hypervirulence plasmids but was highly similar to a plasmid harbored by a swine isolate KPCTRSRTH01_p2 collected in Thailand in 2016 (Fig 5A & Table 1). For comparison, we included in the analysis pTK421_2, a unique hvKP plasmid we had previously identified from a bloodstream isolate collected at NMH in 2013 (35). pTK421_2 contains PAL-1, PAL-2, and conjugation genes (Fig 1). This plasmid was also distinct from pK2044 or KP52.145pII (Fig 4A & S5). We therefore aligned pTK421_2 to pKPN23_1 but found that these plasmids shared relatively little alignment beyond PAL-1 (Fig 5B). Overall, among the 104 *K. pneumoniae* bloodstream isolates, we identified four isolates that contained two distinct hypervirulence plasmids and a fifth isolate that contained a plasmid containing aerobactin biosynthetic genes.

Phylogenetic analysis of bloodstream isolates containing hvKP pathogenicity loci

To examine the phylogenetic relationships of the five NMH bloodstream isolates containing aerobactin biosynthesis genes, we generated a core genome phylogenetic tree of these isolates along with previously published hvKP isolates. These results confirmed previous findings that KL1 hvKP isolates tend to be phylogenetically clustered, whereas KL2 hvKP isolates tend to be more dispersed (Fig S6). Neither ST23-K1 isolate is part of a previously described and globally distributed CG23-I clade and, as such, neither contained the combination of yersiniabactin and colibactin biosynthetics genes

observed in *ICEKp10* (Fig S6) (18). KPN49 is part of a rarely described ST66-K2 lineage consistent with the recent global re-emergence of this clone (Fig S6) (56, 59, 60).

Although KPN165 and KPN49 both harbor KL2 capsule loci and very similar KP52.145pII-like plasmids (99.6% identify) containing additional putative conjugation loci, they are quite divergent genetically (Fig 4B, S6, & Table 1). These findings suggest that this plasmid, which contains a number of virulence genes, has spread by horizontal transmission. Together, these results suggest that nonclonal strains with features of hypervirulent *K. pneumoniae* are circulating at NMH.

Pathogenesis in a murine model of pneumonia

Studies to date suggest that hvKP strains share the common feature of being highly virulent in mouse models of infection. To more definitively determine whether the isolates with features of hvKP were indeed hypervirulent, we measured the virulence of representative isolates in a mouse pneumonia model. To determine the level of virulence of the isolates containing characteristics of hvKP, 50% lethal dose (LD_{50}) measurements were made. For reference, we first determined the virulence of a published hvKP isolate, hvKP5, which is an ST23 KL1 strain that harbors *iuc1, iro1, rmpA,* a disrupted allele of *rmpA2,* and is hmv (44). As expected, hvKP5 was extremely virulent and had a LD_{50} of $10^{2.0}$ CFU. In this model hvKP5 was more virulent than previously published hvKP isolates, hvKP1 and hvKP4, which have an LD_{50} of $10^{3.2}$ and $10^{4.6}$ CFU, respectively (Fig 6A) (57). From our collection, we selected KPN8 and KPN49 as representative pK2044 KP52.145pII isolates, respectively. These isolates had LD_{50} values of $10^{2.2}$ and $10^{1.5}$ CFU, respectively, indicating high levels of virulence (Fig 6C & 6E). In comparison, KPN23, which is non-hmv and has an *iuc3* virulence plasmid lacking other hvKP

virulence genes, had an intermediate LD_{50} value of $10^{6.1}$ CFU (Fig 6D). We also included in the analysis TK421, the hvKP-like strain that we had previously identified that contained *iuc2, iro2, rmpA,* and was hmv (Table 1). TK421 had an LD_{50} of $10^{4.5}$ CFU (Fig 6B). Finally, as a control we tested KPN80, an hmv blood stream isolate from our collection lacking *iuc, iro, rmpA,* and *rmpA2* genes (Table 1) (35, 44). KPN80 had an LD_{50} value of $10^{8.1}$ CFU which is consistent with previously published LD_{50} values for cKP (Fig 6F) (57). Collectively, these data confirm that KPN8, KPN49, and TK421 are hvKP strains and suggest that KPN115 and KPN165 are also hvKP. KPN23 had an intermediate pathogenic phenotype and is more virulent than a cKP strain but less virulent than typical hvKP strains. In addition, these findings indicate that there is a spectrum of virulence among hvKP isolates. These data suggest that multiple factors are necessary for full virulence and that *iuc* genes or a hmv phenotype alone is not sufficient to define an isolate as hypervirulent.

Infections caused by hvKP strains

Since KPN8, KPN49, KPN115, and KPN165 had microbiological, genetic, and virulence properties of hvKP, we next examined the clinical context of the infections they caused. None of the patients infected by these strains had known travel history to areas where hvKP is endemic. Three of the four patients had infections that were community-acquired. Two infections led to hepatic abscesses, and one infection resulted in a lung abscess (Table 3). Two infections occurred in patients with diabetes mellitus, a known risk factor for hvKP (Table 3) (61-63). None of the patients had other common manifestations of hvKP infections, such as endophthalmitis, meningitis, or necrotizing fasciitis. We also looked at the infections cause by KPN23, KPN80, and TK421. The

patient infected with TK421, a slightly less virulent strain with features of hvKP, had a history of diabetes mellitus and presented with a community-acquired liver abscess, although this patient had predisposing conditions including a previous Whipple procedure and a history of prior liver abscesses. The patient infected with KPN23, the *iuc3*+, non-hmv strain with somewhat lower virulence, did not have features of or risk factors for hvKP infection. Likewise, the patient infected with KPN80, the hmv isolate that lacked hvKP-associated genes, also did not have features of or risk factors for hvKP infection. Although the very small number of patients prevents conclusions from being drawn, the characteristics of these infections support the assertion that hvKP strains are circulating at NMH.

Discussion

K. pneumoniae bloodstream isolates at NMH had significant diversity in sequence type, capsule type, antimicrobial resistance genes, and virulence factors. In total, there were 75 distinct sequence types in our collection, demonstrating that a broad spectrum of the *K. pneumoniae* species has the potential to cause invasive infections. Nearly all of these isolates (n=100, 96%) were cKP (i.e. lacked genetic features of hvKP, and a substantial proportion of these were MDR or XDR (n=17, 16.3% and n=12, 11.5%, respectively) and 9 (8.7%) were resistant to carbapenems. A substantial number of the isolates belonged to the established global high-risk clones including ST258, ST45, ST23, ST15, ST66, and ST147. However, 4 (3.8%) of the isolates had genetic, phenotypic, and virulence features consistent with hvKP, indicating that hvKP strains are circulating in the U.S. community. These four isolates belonged to the established hvKP ST23 and ST380 lineages and the reemerging ST66 lineage. These findings indicate

that antibiotic-resistant and high-risk clones comprise a substantial number of *K. pneumoniae* causing bloodstream infections at NMH but that hvKP strains are also present.

In MDR cKP infections, delay in administration of active antimicrobial therapy may lead to poor outcomes (64, 65), and it therefore important to know the prevalence of these infections. Two large studies have recently evaluated the molecular characteristics of either extended spectrum beta-lactamase resistant or carbapenem resistant isolates from U.S. hospitalized patients (from 2011-2017) and ST258 and ST307 are found at exceptionally high rates, 26.7-64.4% and 7.4-35.7%, respectively (66, 67). A recent study from our group showed that at NMH 74.1% of carbapenem resistant isolates are ST258 (68). Among bloodstream isolates at NMH, 17 (16.3%) isolates were resistant to three or more classes of antibiotics and considered MDR-cKP, 12 (11.5%) isolates were ESBL producing (12%). Comparatively, ESBL prevalence among collections from Asia ranges from 12-79% (69-73). Carbapenamases were found in 9% of isolates, with most strains carrying bla_{KPC-3} and one strain carrying bla_{NDM-1}. As expected, ST258 (n=6, 5.7%) and ST307 (n=2, 1.9%) were both identified in our collection.

The invasive nature of hvKP strains allow them to cause unusual infections such as PLA, endogenous endophthalmitis, necrotizing fasciitis, and meningitis associated with clinical implications distinct from those of the more common cKP strains (33). For example, 9-18% of PLA patients have a recurrence of their infection (74, 75), suggesting that prolonged treatment courses may be necessary. In one study, 10 of 14 patients with endogenous endophthalmitis progressed to blindness (76), underscoring that these infections are medical emergencies. hvKP strains are prone to disseminate, and culture of an hvKP isolate from, for example, a liver abscess may prompt a search for other foci of metastatic infection. It therefore can be argued that hvKP isolates should be identified

as such by hospital laboratories and that the prevalence of these isolates should be studied. Our finding that 3.8% of *K. pneumoniae* bloodstream isolates at NMH were hvKP agrees with two published U.S. surveillance studies, which describe the hvKp prevalence as 3.7%-6.3% of *K. pneumoniae* infections in two U.S. cities. In 2010, 64 *K. pneumoniae* strains were analyzed from two hospitals in the greater Houston area (25). They identified four strains (6.3%) containing hvKp pathogenicity-associated genes, based on the presence of *rmpA* and K1 capsule type by PCR amplification. In 2018, a larger study in New York City characterized *K. pneumoniae* isolates from 462 patients (24). This study identified 17 (3.7%) isolates by PCR amplification that contained the hvKp biomarkers *rmpA* and *iucA*. In contrast, a 2013 report from China, where hvKP is endemic, described an hvKP prevalence of 37.8%, (defined by the presence of the *iuc* gene) (77). A recent genomic surveillance study of seven countries in South and Southeast Asia analyzed the sequences of 365 *K. pneumoniae* bloodstream isolates collected from 2010-2017 (78). Sequencing revealed that 26% (95/365) were *iuc*+, 17% (63/365) were *iuc*+ and either *rmpA*+ or *rmpA2*+, and an additional 0.8% (3/365) were *iro*+ and *rmpA*+. Alarmingly, of the *iuc*+ isolates 13.7% (13/95) contained carbapenamase genes, but only 1 was positive for multiple hvKp factors (*iuc*, *rmpA/2*) and a carbapenamase gene. Thus far, antimicrobial-resistant hvKp infections are rare in the United States, and none of the *iuc*+ isolates identified at NMH contained accessory antimicrobial resistance genes. However, antimicrobial-resistant hvKp infections are on the rise in Asia, likely due to the increase in hospital-acquired hvKp infections (79-81). Our results together with these reports indicate call attention to the need for further studies evaluating the prevalence and clinical implications of hvKP infections in the United States and other countries outside of Asia.

Since hvKp pathogenicity loci are normally encoded on large plasmids, we performed long-read sequencing of the isolates that contained *iucA*. Four of these isolates harbored a plasmid similar to one of the two previously described hvKp virulence plasmids, pK2044 or KP52.145pII (28-30). The plasmids from these four isolates contained multiple hvKP-associated genetic loci (*iuc, iro,* and *rmpA*), and the isolates that harbored them had hmv phenotypes and LD_{50} values consistent with hvKp (Fig 6 and Table 1). Among these, three isolates (KPN49, KPN115, and KPN165) caused severe community-acquired infections with abscess formation (2 hepatic and 1 lung). Taken together, these data indicate that these four isolates are indeed hvKP and that multiple strains of hvKp with distinct plasmids are circulating at NMH.

A closer examination of the isolates and plasmids provided several additional insights into hvKP. For example, the KP52.145pII-like plasmids of KPN49 and KPN165 contained a 40 kb insert containing putative conjugation genes, suggesting that these plasmids, unlike typical hypervirulence plasmids, were capable of transmission. Indeed, the two isolates that contained these plasmids, KPN49 and KPN165, were phylogenetically distinct (ST66 and ST380, Fig S6), consistent with horizontal dissemination of this plasmid. We identified a number of isolates that were hmv but did not have other features of hvKP. One of these isolates, KPN80, was tested in the mouse model and was found to have a very low level of virulence. These findings agree with previous reports indicating that hypermucoviscosity does not accurately predict hvKP (48, 55). In addition to the four hvKP isolates, we identified one additional isolate, KPN23, that harbored a unique plasmid containing the aerobactin biosynthesis locus but not other hvKP-associated virulence genes. This isolate was not hmv, and it caused a typical cKP disease: a hospital-acquired infection in a patient with pancreatic cancer that was not associated with abscess formation. However, it was associated with a level of

virulence in the mouse model that was intermediate between hvKP and cKP. These findings suggest that *K. pneumoniae* strains may not fall neatly into either the cKP or the hvKP classification but may have intermediate phenotypes.

Conclusions

In this study, *Klebsiella spp*. bloodstream isolates at NMH were collected consecutively from 2015-2017. Whole genome sequencing revealed that these isolates are diverse in sequence type, capsule type, and virulence gene content. 30.7% of isolates were high-risk clones, predominantly ST258 and ST45, whereas 3.8% of isolates were hvKP belonging to ST23, ST66, and ST380.

Materials and Methods

Bacterial isolates and growth conditions

The isolates used in this study were from consecutive blood cultures collected between April 2015-April 2017 with growth designated as *K. pneumoniae* by the NMH Clinical Microbiology Laboratory using a VITEK-2 platform (82). For the sub-analysis of isolates determined to be *K. pneumoniae* by sequencing, only the first isolate cultured from each unique infection was included. For experiments, bacteria were grown at 37°C in lysogeny broth (LB) or on LB agar plates.

Whole-Genome Sequencing

Genomic DNA was prepared from a single colony cultured overnight at 37°C in LB using the Maxwell 16 system (Promega Corp., Madison, WI). Libraries for Illumina sequencing were prepared using either Nextera XT (Illumina, Inc., San Diego, CA) or

Seqwell (Seqwell, Massachusetts) library kits and sequenced on an Illumina MiSeq or NextSeq 500 instrument to generate paired-end 300 bp or 150 bp reads (Table S3). Reads were trimmed using Trimmomatic (v0.36) and *de novo* assembly was performed using SPAdes version 3.9.1 (83, 84). Nanopore sequencing was performed as described previously (85, 86). Briefly, libraries were prepared from genomic DNA using the ligation sequencing kit (SQK-LSK109, Oxford Nanopore, UK). Libraries were sequenced on the MinION using a FLO-MIN106 flow cell and base calling and demultiplexing of sequence reads was performed using Guppy v3.4.5 (87). Hybrid assembly and circularization of Nanopore and Illumina reads were performed using Flye v2.9. Flye assembly information is included in Table S4. Nanopore sequencing errors were corrected by aligning Illumina reads to the assembly using BWA v0.7.17 and correcting the errors with serial rounds of Pilon v1.23. Annotation was performed using the NCBI Prokaryotic Genome Annotation Pipeline (88).

Hypermucoviscosity testing

The string test was performed as described previously (89). Isolates were grown overnight at 37°C on LB agar. A single colony was lifted with a loop to evaluate the formation of a viscous string between the loop and the colony. A positive string test was defined as a string length ≥ 5 mm. A centrifugation assay was also used to assess hypermucoviscosity. Centrifugation of overnight bacterial cultures (5 mL LB). was performed at 3,220 x g (RCF) for 10 minutes (55). Hypermucoviscous isolates were identified qualitatively by the persistence of turbidity.

Tellurite resistance testing

For screening of tellurite resistance, *K. pneumoniae* was grown at 37°C on LB agar plates supplemented with 3 μg/mL potassium tellurite (Sigma-Aldrich, USA).

Phylogenetic analysis

FastTree 2 was used to estimate a maximum-likelihood phylogenetic tree (90). Core SNPs were determined by aligning raw Illumina reads to the reference strain (NTUH-K2044) using bwa-0.7.15 and filtering them to 95% core. The phylogenetic tree was visualized and annotated using iTOL (v4)(91).

Molecular typing and identification of virulence genes

Assembled whole genome sequences were analyzed with the bioinformatics tools *Kleborate* v2.1 and *Kaptive* v0.7.3 to evaluate multilocus sequence type, capsule locus typing, antimicrobial resistance genes, and virulence gene content (31, 92). Plasmids identified by whole genome sequencing were aligned using BLAST Ring Image generator (BRIG) with the alignment threshold set at 85% identity (93). Plasmid replicons were identified using the PlasmidFinder v2.1 online database (94).

Animal Studies

Anesthetized 6- to 8-week-old C57BL/6 female mice purchased from Jackson Labs were infected intranasally as described previously (48). Briefly, sets of mice were infected with different doses and monitored for two weeks post-infection for pre-lethal illness. Strain dosing, deaths, and total mice inoculated are included in Table S2. LD_{50} values were determined in R, with the *drc* package (95). To minimize pain and distress in the animals, mice were euthanized when they reached predetermined endpoints of >20% weight loss, abnormal respiratory rate, or a hunched posture with minimal activity. All procedures were performed in accordance with the guidelines approved by the

Northwestern University Animal Care and Use Committee as described in protocol IS00002172.

Statistical Analysis

Statistical analysis was performed using GraphPad Prism. Student T-test and analysis of variance (ANOVA) followed by the Bonferroni's correction for multiple comparisons were performed for parametric variables. For non-parametric variables, the Mann-Whitney U test was used. For comparison of survival curves, the Mantel-Cox log rank test was used. Simpson Diversity index was determined in R using the package 'vegan'.

Declarations

Ethics, consent and permissions

Patient Chart Review

The following information was extracted retrospectively from the electronic medical records of patients from which the blood cultures were obtained: antibiotic susceptibility (as determined by the NMH Clinical Microbiology Laboratory using a VITEK-2 platform), age, type of infection, medical comorbidities, travel history, and community vs. hospital acquisition of the *K. pneumoniae* infection (i.e. onset prior to 48 hr of hospitalization or after 48 hr of hospitalization). Clinical breakpoints used to categorize isolates as resistant, intermediate, or susceptible are described for each antibiotic in Table S1. All data were collected as part of routine diagnostic care and all samples and data have been de-identified and pose no more than minimal risk to subjects. This study was approved and granted a waiver of the consent process by the Northwestern Institutional Review Board under protocol STU00211033.

Consent to publish

Not applicable

Availability of data and materials

The whole-genome assemblies have been deposited at GenBank under BioProject number PRJNA788509. Assembly accession numbers are included in Table S3. MIC and *Kleborate* data are included in Table S1.

Competing interests

The authors declare that they have no competing interests.

Funding

Travis Kochan has acquired funding from the American Heart Association (837089) and the National Institute of Health under T32 AI007476. Alan Hauser has acquired funding from National Institutes of Health during the conduct of this study: R01 AI118257, R21 AI153953 K24 AI104831, and R21 AI164254. Rachel Medernach has acquired funding from National Institute of Health under T32 AI095207. The funding sources had no influence on the design of the study and collection, analysis, interpretation of data, and writing of the manuscript.

Authors' contributions

TK and AH designed the study. TK, SN, BC, SG, MLC SM, and NK performed the phenotypic experiments. TK and EO performed the computational analyses. RM and BC analyzed and interpreted the patient data. FK and CQ collected and identified the isolates as *Klebsiella spp*. TK, SN, SM, EO, and AR analyzed the data. TK and AH wrote

the paper, and all other authors contributed to the writing. All authors read and approved the final version of the manuscript.

Bibliography

1. Podschun R, Ullmann U. 1998. *Klebsiella* spp. as nosocomial pathogens: epidemiology, taxonomy, typing methods, and pathogenicity factors. Clin Microbiol Rev 11:589-603.
2. Dhesi Z, Enne VI, Brealey D, Livermore DM, High J, Russell C, Colles A, Kandil H, Mack D, Martin D, Page V, Parker R, Roulston K, Singh S, Wey E, Swart AM, Stirling S, Barber JA, O'Grady J, Gant VA. 2020. Organisms causing secondary pneumonias in COVID-19 patients at 5 UK ICUs as detected with the FilmArray test doi:doi: https://doi.org/10.1101/2020.06.22.20131573, medRvix.
3. Paczosa MK, Mecsas J. 2016. *Klebsiella pneumoniae*: Going on the Offense with a Strong Defense. Microbiol Mol Biol Rev 80:629-61.
4. Lawlor MS, Hsu J, Rick PD, Miller VL. 2005. Identification of *Klebsiella pneumoniae* virulence determinants using an intranasal infection model. Mol Microbiol 58:1054-73.
5. Russo TA, Marr CM. 2019. Hypervirulent *Klebsiella pneumoniae*. Clin Microbiol Rev 32.
6. Marcade G, Brisse S, Bialek S, Marcon E, Leflon-Guibout V, Passet V, Moreau R, Nicolas-Chanoine MH. 2013. The emergence of multidrug-resistant *Klebsiella pneumoniae* of international clones ST13, ST16, ST35, ST48 and ST101 in a teaching hospital in the Paris region. Epidemiol Infect 141:1705-12.
7. Meng X, Yang J, Duan J, Liu S, Huang X, Wen X, Huang X, Fu C, Li J, Dou Q, Liu Y, Wang J, Yan Q, Zou M, Liu W, Peng Z, Chen L, Li C, Wu A. 2019. Assessing Molecular Epidemiology of Carbapenem-resistant *Klebsiella pneumoniae* (CR-KP) with MLST and MALDI-TOF in Central China. Sci Rep 9:2271.
8. Roulston KJ, Bharucha T, Turton JF, Hopkins KL, Mack DJF. 2018. A case of NDM-carbapenemase-producing hypervirulent *Klebsiella pneumoniae* sequence type 23 from the UK. JMM Case Rep 5:e005130.
9. Shen D, Ma G, Li C, Jia X, Qin C, Yang T, Wang L, Jiang X, Ding N, Zhang X, Yue L, Yin Z, Zeng L, Zhao Y, Zhou D, Chen F. 2019. Emergence of a Multidrug-Resistant Hypervirulent *Klebsiella pneumoniae* Sequence Type 23 Strain with a Rare bla CTX-M-24-Harboring Virulence Plasmid. Antimicrob Agents Chemother 63.
10. Shu L, Dong N, Lu J, Zheng Z, Hu J, Zeng W, Sun Q, Chan EW, Zhou H, Hu F, Chen S, Zhang R. 2019. Emergence of OXA-232 Carbapenemase-Producing *Klebsiella pneumoniae* That Carries a pLVPK-Like Virulence Plasmid among Elderly Patients in China. Antimicrob Agents Chemother 63.

605 11. Lester CH, Olsen SS, Jakobsen L, Arpi M, Fuursted K, Hansen DS, Heltberg O,
606 Holm A, Hojbjerg T, Jensen KT, Johansen HK, Justesen US, Kemp M, Knudsen
607 JD, Roder B, Frimodt-Moller N, Hammerum AM. 2011. Emergence of
608 extended-spectrum beta-lactamase (ESBL)-producing *Klebsiella pneumoniae*
609 in Danish hospitals; this is in part explained by spread of two CTX-M-15
610 clones with multilocus sequence types 15 and 16 in Zealand. Int J Antimicrob
611 Agents 38:180-2.
612 12. Navon-Venezia S, Kondratyeva K, Carattoli A. 2017. *Klebsiella pneumoniae*: a
613 major worldwide source and shuttle for antibiotic resistance. FEMS Microbiol
614 Rev 41:252-275.
615 13. Tacconelli E, Magrini N. 2017. Global priority list of antibiotic-resistant
616 bacteria to guide research, discovery, and development of new antibiotics.
617 https://www.who.int/medicines/publications/WHO-PPL-
618 Short_Summary_25Feb-ET_NM_WHO.pdf. Accessed October 2.
619 14. Talbot GH, Bradley J, Edwards JE, Jr., Gilbert D, Scheld M, Bartlett JG. 2006.
620 Bad bugs need drugs: an update on the development pipeline from the
621 Antimicrobial Availability Task Force of the Infectious Diseases Society of
622 America. Clin Infect Dis 42:657-668.
623 15. CDC. 2013. Antibiotic resistance threats in the United States, 2013.
624 http://www.cdc.gov/drugresistance/threat-report-2013/. Accessed
625 September 18.
626 16. Liu YC, Cheng DL, Lin CL. 1986. *Klebsiella pneumoniae* liver abscess
627 associated with septic endophthalmitis. Arch Intern Med 146:1913-6.
628 17. Fang FC, Sandler N, Libby SJ. 2005. Liver abscess caused by magA+ *Klebsiella*
629 *pneumoniae* in North America. J Clin Microbiol 43:991-2.
630 18. Lam MMC, Wyres KL, Duchene S, Wick RR, Judd LM, Gan YH, Hoh CH,
631 Archuleta S, Molton JS, Kalimuddin S, Koh TH, Passet V, Brisse S, Holt KE.
632 2018. Population genomics of hypervirulent *Klebsiella pneumoniae* clonal-
633 group 23 reveals early emergence and rapid global dissemination. Nat
634 Commun 9:2703.
635 19. Turton JF, Englender H, Gabriel SN, Turton SE, Kaufmann ME, Pitt TL. 2007.
636 Genetically similar isolates of *Klebsiella pneumoniae* serotype K1 causing
637 liver abscesses in three continents. J Med Microbiol 56:593-7.
638 20. Siu LK, Fung CP, Chang FY, Lee N, Yeh KM, Koh TH, Ip M. 2011. Molecular
639 typing and virulence analysis of serotype K1 *Klebsiella pneumoniae* strains
640 isolated from liver abscess patients and stool samples from noninfectious
641 subjects in Hong Kong, Singapore, and Taiwan. J Clin Microbiol 49:3761-5.
642 21. Vila A, Cassata A, Pagella H, Amadio C, Yeh KM, Chang FY, Siu LK. 2011.
643 Appearance of *Klebsiella pneumoniae* liver abscess syndrome in Argentina:
644 case report and review of molecular mechanisms of pathogenesis. Open
645 Microbiol J 5:107-13.
646 22. Pastagia M, Arumugam V. 2008. *Klebsiella pneumoniae* liver abscesses in a
647 public hospital in Queens, New York. Travel Med Infect Dis 6:228-33.
648 23. Rahimian J, Wilson T, Oram V, Holzman RS. 2004. Pyogenic liver abscess:
649 recent trends in etiology and mortality. Clin Infect Dis 39:1654-9.

650 24. Parrott AM, Shi J, Aaron J, Green DA, Whittier S, Wu F. 2020. Detection of
651 multiple hypervirulent *Klebsiella pneumoniae* strains in a New York City
652 hospital through screening of virulence genes. Clin Microbiol Infect
653 doi:10.1016/j.cmi.2020.05.012.
654 25. Chou A, Nuila RE, Franco LM, Stager CE, Atmar RL, Zechiedrich L. 2016.
655 Prevalence of hypervirulent *Klebsiella pneumoniae*-associated genes rmpA
656 and magA in two tertiary hospitals in Houston, TX, USA. J Med Microbiol
657 65:1047-8.
658 26. Peirano G, Pitout JD, Laupland KB, Meatherall B, Gregson DB. 2013.
659 Population-based surveillance for hypermucoviscosity *Klebsiella pneumoniae*
660 causing community-acquired bacteremia in Calgary, Alberta. Can J Infect Dis
661 Med Microbiol 24:e61-4.
662 27. Russo TA, Olson R, Fang CT, Stoesser N, Miller M, MacDonald U, Hutson A,
663 Barker JH, La Hoz RM, Johnson JR. 2018. Identification of Biomarkers for
664 Differentiation of Hypervirulent *Klebsiella pneumoniae* from Classical K.
665 *pneumoniae*. J Clin Microbiol 56.
666 28. Chen YT, Chang HY, Lai YC, Pan CC, Tsai SF, Peng HL. 2004. Sequencing and
667 analysis of the large virulence plasmid pLVPK of *Klebsiella pneumoniae* CG43.
668 Gene 337:189-98.
669 29. Nassif X, Fournier JM, Arondel J, Sansonetti PJ. 1989. Mucoid phenotype of
670 *Klebsiella pneumoniae* is a plasmid-encoded virulence factor. Infect Immun
671 57:546-52.
672 30. Wu KM, Li LH, Yan JJ, Tsao N, Liao TL, Tsai HC, Fung CP, Chen HJ, Liu YM,
673 Wang JT, Fang CT, Chang SC, Shu HY, Liu TT, Chen YT, Shiau YR, Lauderdale
674 TL, Su IJ, Kirby R, Tsai SF. 2009. Genome sequencing and comparative
675 analysis of *Klebsiella pneumoniae* NTUH-K2044, a strain causing liver abscess
676 and meningitis. J Bacteriol 191:4492-501.
677 31. Lam MMC, Wyres KL, Judd LM, Wick RR, Jenney A, Brisse S, Holt KE. 2018.
678 Tracking key virulence loci encoding aerobactin and salmochelin
679 siderophore synthesis in *Klebsiella pneumoniae*. Genome Med 10:77.
680 32. Wyres KL, Wick RR, Judd LM, Froumine R, Tokolyi A, Gorrie CL, Lam MMC,
681 Duchene S, Jenney A, Holt KE. 2019. Distinct evolutionary dynamics of
682 horizontal gene transfer in drug resistant and virulent clones of *Klebsiella*
683 *pneumoniae*. PLoS Genet 15:e1008114.
684 33. Shon AS, Bajwa RP, Russo TA. 2013. Hypervirulent (hypermucoviscous)
685 *Klebsiella pneumoniae*: a new and dangerous breed. Virulence 4:107-18.
686 34. Lery LM, Frangeul L, Tomas A, Passet V, Almeida AS, Bialek-Davenet S, Barbe
687 V, Bengoechea JA, Sansonetti P, Brisse S, Tournebize R. 2014. Comparative
688 analysis of *Klebsiella pneumoniae* genomes identifies a phospholipase D
689 family protein as a novel virulence factor. BMC Biol 12:41.
690 35. Kochan TJ, Ozer EA, Pincus NB, Fitzpatrick MA, Hauser AR. 2020. Complete
691 Genome Sequence of *Klebsiella pneumoniae* Strain TK421, a Conjugative
692 Hypervirulent Isolate. Microbiol Resour Announc 9.
693 36. Hsieh PF, Lin TL, Lee CZ, Tsai SF, Wang JT. 2008. Serum-induced iron-
694 acquisition systems and TonB contribute to virulence in *Klebsiella*

695 *pneumoniae* causing primary pyogenic liver abscess. J Infect Dis 197:1717-
696 27.
697 37. Russo TA, Olson R, MacDonald U, Beanan J, Davidson BA. 2015. Aerobactin,
698 but not yersiniabactin, salmochelin, or enterobactin, enables the
699 growth/survival of hypervirulent (hypermucoviscous) *Klebsiella pneumoniae*
700 ex vivo and in vivo. Infect Immun 83:3325-33.
701 38. Xiong H, Carter RA, Leiner IM, Tang YW, Chen L, Kreiswirth BN, Pamer EG.
702 2015. Distinct Contributions of Neutrophils and CCR2+ Monocytes to
703 Pulmonary Clearance of Different *Klebsiella pneumoniae* Strains. Infect
704 Immun 83:3418-27.
705 39. Bachman MA, Oyler JE, Burns SH, Caza M, Lepine F, Dozois CM, Weiser JN.
706 2011. *Klebsiella pneumoniae* yersiniabactin promotes respiratory tract
707 infection through evasion of lipocalin 2. Infect Immun 79:3309-16.
708 40. Merlet A, Cazanave C, Dutronc H, de Barbeyrac B, Brisse S, Dupon M. 2012.
709 Primary liver abscess due to CC23-K1 virulent clone of *Klebsiella pneumoniae*
710 in France. Clin Microbiol Infect 18:E338-9.
711 41. Patel PK, Russo TA, Karchmer AW. 2014. Hypervirulent *Klebsiella*
712 *pneumoniae*. Open Forum Infect Dis 1:ofu028.
713 42. Pomakova DK, Hsiao CB, Beanan JM, Olson R, MacDonald U, Keynan Y, Russo
714 TA. 2012. Clinical and phenotypic differences between classic and
715 hypervirulent *Klebsiella* pneumonia: an emerging and under-recognized
716 pathogenic variant. Eur J Clin Microbiol Infect Dis 31:981-9.
717 43. Russo TA, Shon AS, Beanan JM, Olson R, MacDonald U, Pomakov AO,
718 Visitacion MP. 2011. Hypervirulent *K. pneumoniae* secretes more and more
719 active iron-acquisition molecules than "classical" *K. pneumoniae* thereby
720 enhancing its virulence. PLoS One 6:e26734.
721 44. Sachdev DD, Yin MT, Horowitz JD, Mukkamala SK, Lee SE, Ratner AJ. 2013.
722 *Klebsiella pneumoniae* K1 liver abscess and septic endophthalmitis in a U.S.
723 resident. J Clin Microbiol 51:1049-51.
724 45. Shon AS, Russo TA. 2012. Hypervirulent *Klebsiella pneumoniae*: the next
725 superbug? Future Microbiol 7:669-71.
726 46. Fang CT, Chuang YP, Shun CT, Chang SC, Wang JT. 2004. A novel virulence
727 gene in *Klebsiella pneumoniae* strains causing primary liver abscess and
728 septic metastatic complications. J Exp Med 199:697-705.
729 47. Lee CH, Liu JW, Su LH, Chien CC, Li CC, Yang KD. 2010. Hypermucoviscosity
730 associated with *Klebsiella pneumoniae*-mediated invasive syndrome: a
731 prospective cross-sectional study in Taiwan. Int J Infect Dis 14:e688-92.
732 48. Krapp F, Morris AR, Ozer EA, Hauser AR. 2017. Virulence Characteristics of
733 Carbapenem-Resistant *Klebsiella pneumoniae* Strains from Patients with
734 Necrotizing Skin and Soft Tissue Infections. Sci Rep 7:13533.
735 49. Harada S, Doi Y. 2018. Hypervirulent *Klebsiella pneumoniae*: a Call for
736 Consensus Definition and International Collaboration. J Clin Microbiol 56.
737 50. Holt KE, Wertheim H, Zadoks RN, Baker S, Whitehouse CA, Dance D, Jenney A,
738 Connor TR, Hsu LY, Severin J, Brisse S, Cao H, Wilksch J, Gorrie C, Schultz MB,
739 Edwards DJ, Nguyen KV, Nguyen TV, Dao TT, Mensink M, Minh VL, Nhu NT,

740 Schultsz C, Kuntaman K, Newton PN, Moore CE, Strugnell RA, Thomson NR.
741 2015. Genomic analysis of diversity, population structure, virulence, and
742 antimicrobial resistance in *Klebsiella pneumoniae*, an urgent threat to public
743 health. Proc Natl Acad Sci U S A 112:E3574-81.
744 51. Lam MMC, Wick RR, Wyres KL, Gorrie CL, Judd LM, Jenney AWJ, Brisse S, Holt
745 KE. 2018. Genetic diversity, mobilisation and spread of the yersiniabactin-
746 encoding mobile element ICEKp in *Klebsiella pneumoniae* populations.
747 Microb Genom 4.
748 52. Lawlor MS, O'Connor C, Miller VL. 2007. Yersiniabactin is a virulence factor
749 for *Klebsiella pneumoniae* during pulmonary infection. Infect Immun
750 75:1463-72.
751 53. Marsh JW, Mustapha MM, Griffith MP, Evans DR, Ezeonwuka C, Pasculle AW,
752 Shutt KA, Sundermann A, Ayres AM, Shields RK, Babiker A, Cooper VS, Van
753 Tyne D, Harrison LH. 2019. Evolution of Outbreak-Causing Carbapenem-
754 Resistant *Klebsiella pneumoniae* ST258 at a Tertiary Care Hospital over 8
755 Years. mBio 10.
756 54. Yu WL, Lee MF, Tang HJ, Chang MC, Chuang YC. 2015. Low prevalence of
757 rmpA and high tendency of rmpA mutation correspond to low virulence of
758 extended spectrum beta-lactamase-producing *Klebsiella pneumoniae* isolates.
759 Virulence 6:162-72.
760 55. Walker KA, Miller VL. 2020. The intersection of capsule gene expression,
761 hypermucoviscosity and hypervirulence in *Klebsiella pneumoniae*. Curr Opin
762 Microbiol 54:95-102.
763 56. Rodrigues C, d'Humieres C, Papin G, Passet V, Ruppe E, Brisse S. 2020.
764 Community-acquired infection caused by the uncommon hypervirulent
765 *Klebsiella pneumoniae* ST66-K2 lineage. Microb Genom 6.
766 57. Agard MJ, Ozer EA, Morris AR, Piseaux R, Hauser AR. 2019. A Genomic
767 Approach To Identify *Klebsiella pneumoniae* and *Acinetobacter baumannii*
768 Strains with Enhanced Competitive Fitness in the Lungs during Multistrain
769 Pneumonia. Infect Immun 87.
770 58. Russo TA, Olson R, Macdonald U, Metzger D, Maltese LM, Drake EJ, Gulick AM.
771 2014. Aerobactin mediates virulence and accounts for increased siderophore
772 production under iron-limiting conditions by hypervirulent
773 (hypermucoviscous) *Klebsiella pneumoniae*. Infect Immun 82:2356-67.
774 59. Kamau E, Allyn PR, Beaird OE, Ward KW, Kwan N, Garner OB, Yang S. 2021.
775 Endogenous Endophthalmitis Caused by ST66-K2 Hypervirulent *Klebsiella*
776 *pneumoniae*, United States. Emerg Infect Dis 27:2215-2218.
777 60. Klaper K, Wendt S, Lubbert C, Lippmann N, Pfeifer Y, Werner G. 2021.
778 Hypervirulent *Klebsiella pneumoniae* of Lineage ST66-K2 Caused
779 Tonsillopharyngitis in a German Patient. Microorganisms 9.
780 61. Han SH. 1995. Review of hepatic abscess from *Klebsiella pneumoniae*. An
781 association with diabetes mellitus and septic endophthalmitis. West J Med
782 162:220-4.
783 62. Huang CR, Lu CH, Chang HW, Lee PY, Lin MW, Chang WN. 2002. Community-
784 acquired spontaneous bacterial meningitis in adult diabetic patients: an

785 analysis of clinical characteristics and prognostic factors. Infection 30:346-
786 50.
787 63. Wang JH, Liu YC, Lee SS, Yen MY, Chen YS, Wang JH, Wann SR, Lin HH. 1998.
788 Primary liver abscess due to *Klebsiella pneumoniae* in Taiwan. Clin Infect Dis
789 26:1434-8.
790 64. Lambregts MMC, Wijnakker R, Bernards AT, Visser LG, Cessie SL, Boer MGJ.
791 2020. Mortality after Delay of Adequate Empiric Antimicrobial Treatment of
792 Bloodstream Infection. J Clin Med 9.
793 65. Weiss SL, Fitzgerald JC, Balamuth F, Alpern ER, Lavelle J, Chilutti M,
794 Grundmeier R, Nadkarni VM, Thomas NJ. 2014. Delayed antimicrobial
795 therapy increases mortality and organ dysfunction duration in pediatric
796 sepsis. Crit Care Med 42:2409-17.
797 66. van Duin D, Arias CA, Komarow L, Chen L, Hanson BM, Weston G, Cober E,
798 Garner OB, Jacob JT, Satlin MJ, Fries BC, Garcia-Diaz J, Doi Y, Dhar S, Kaye KS,
799 Earley M, Hujer AM, Hujer KM, Domitrovic TN, Shropshire WC, Dinh A, Manca
800 C, Luterbach CL, Wang M, Paterson DL, Banerjee R, Patel R, Evans S, Hill C,
801 Arias R, Chambers HF, Fowler VG, Jr., Kreiswirth BN, Bonomo RA, Multi-Drug
802 Resistant Organism Network I. 2020. Molecular and clinical epidemiology of
803 carbapenem-resistant Enterobacterales in the USA (CRACKLE-2): a
804 prospective cohort study. Lancet Infect Dis 20:731-741.
805 67. Long SW, Olsen RJ, Eagar TN, Beres SB, Zhao P, Davis JJ, Brettin T, Xia F,
806 Musser JM. 2017. Population Genomic Analysis of 1,777 Extended-Spectrum
807 Beta-Lactamase-Producing *Klebsiella pneumoniae* Isolates, Houston, Texas:
808 Unexpected Abundance of Clonal Group 307. mBio 8.
809 68. Bulman ZP, Krapp F, Pincus NB, Wenzler E, Murphy KR, Qi C, Ozer EA, Hauser
810 AR. 2021. Genomic Features Associated with the Degree of Phenotypic
811 Resistance to Carbapenems in Carbapenem-Resistant *Klebsiella pneumoniae*.
812 mSystems 6:e0019421.
813 69. Dat VQ, Vu HN, Nguyen The H, Nguyen HT, Hoang LB, Vu Tien Viet D, Bui CL,
814 Van Nguyen K, Nguyen TV, Trinh DT, Torre A, van Doorn HR, Nadjm B,
815 Wertheim HFL. 2017. Bacterial bloodstream infections in a tertiary infectious
816 diseases hospital in Northern Vietnam: aetiology, drug resistance, and
817 treatment outcome. BMC Infect Dis 17:493.
818 70. Fox-Lewis A, Takata J, Miliya T, Lubell Y, Soeng S, Sar P, Rith K, McKellar G,
819 Wuthiekanun V, McGonagle E, Stoesser N, Moore CE, Parry CM, Turner C, Day
820 NPJ, Cooper BS, Turner P. 2018. Antimicrobial Resistance in Invasive
821 Bacterial Infections in Hospitalized Children, Cambodia, 2007-2016. Emerg
822 Infect Dis 24:841-851.
823 71. Anderson M, Luangxay K, Sisouk K, Vorlasan L, Soumphonphakdy B,
824 Sengmouang V, Chansamouth V, Phommasone K, Van Dyke R, Chong E, Dance
825 DA, Phetsouvanh R, Newton PN. 2014. Epidemiology of bacteremia in young
826 hospitalized infants in Vientiane, Laos, 2000-2011. J Trop Pediatr 60:10-6.
827 72. Hsu LY, Tan TY, Jureen R, Koh TH, Krishnan P, Tzer-Pin Lin R, Wen-Sin Tee N,
828 Tambyah PA. 2007. Antimicrobial drug resistance in Singapore hospitals.
829 Emerg Infect Dis 13:1944-7.

830 73. Jajoo M, Manchanda V, Chaurasia S, Sankar MJ, Gautam H, Agarwal R, Yadav
831 CP, Aggarwal KC, Chellani H, Ramji S, Deb M, Gaind R, Kumar S, Arya S,
832 Sreenivas V, Kapil A, Mathur P, Rasaily R, Deorari AK, Paul VK, Investigators
833 of the Delhi Neonatal Infection Study collaboration NDI. 2018. Alarming rates
834 of antimicrobial resistance and fungal sepsis in outborn neonates in North
835 India. PLoS One 13:e0180705.
836 74. Wang H, Ren Y, Chang Z, Liu Z. 2020. The increased recurrence rate of liver
837 abscess caused by extended-spectrum beta-lactamase-producing *Klebsiella*
838 *pneumoniae*. Eur J Clin Microbiol Infect Dis 39:1315-1320.
839 75. Siu LK, Yeh KM, Lin JC, Fung CP, Chang FY. 2012. *Klebsiella pneumoniae* liver
840 abscess: a new invasive syndrome. Lancet Infect Dis 12:881-7.
841 76. Chou FF, Kou HK. 1996. Endogenous endophthalmitis associated with
842 pyogenic hepatic abscess. J Am Coll Surg 182:33-6.
843 77. Zhang Y, Zhao C, Wang Q, Wang X, Chen H, Li H, Zhang F, Li S, Wang R, Wang
844 H. 2016. High Prevalence of Hypervirulent *Klebsiella pneumoniae* Infection in
845 China: Geographic Distribution, Clinical Characteristics, and Antimicrobial
846 Resistance. Antimicrob Agents Chemother 60:6115-20.
847 78. Wyres KL, Nguyen TNT, Lam MMC, Judd LM, van Vinh Chau N, Dance DAB, Ip
848 M, Karkey A, Ling CL, Miliya T, Newton PN, Lan NPH, Sengduangphachanh A,
849 Turner P, Veeraraghavan B, Vinh PV, Vongsouvath M, Thomson NR, Baker S,
850 Holt KE. 2020. Genomic surveillance for hypervirulence and multi-drug
851 resistance in invasive *Klebsiella pneumoniae* from South and Southeast Asia.
852 Genome Med 12:11.
853 79. Karlsson M, Stanton RA, Ansari U, McAllister G, Chan MY, Sula E, Grass JE,
854 Duffy N, Anacker ML, Witwer ML, Rasheed JK, Elkins CA, Halpin AL. 2019.
855 Identification of a Carbapenemase-Producing Hypervirulent *Klebsiella*
856 *pneumoniae* Isolate in the United States. Antimicrob Agents Chemother 63.
857 80. Liu C, Du P, Xiao N, Ji F, Russo TA, Guo J. 2020. Hypervirulent *Klebsiella*
858 *pneumoniae* is emerging as an increasingly prevalent K. *pneumoniae*
859 pathotype responsible for nosocomial and healthcare-associated infections in
860 Beijing, China. Virulence 11:1215-1224.
861 81. Li J, Ren J, Wang W, Wang G, Gu G, Wu X, Wang Y, Huang M, Li J. 2018. Risk
862 factors and clinical outcomes of hypervirulent *Klebsiella pneumoniae* induced
863 bloodstream infections. Eur J Clin Microbiol Infect Dis 37:679-689.
864 82. Leverstein-van Hall MA, Fluit AC, Paauw A, Box AT, Brisse S, Verhoef J. 2002.
865 Evaluation of the Etest ESBL and the BD Phoenix, VITEK 1, and VITEK 2
866 automated instruments for detection of extended-spectrum beta-lactamases
867 in multiresistant *Escherichia coli* and *Klebsiella* spp. J Clin Microbiol 40:3703-
868 11.
869 83. Bolger AM, Lohse M, Usadel B. 2014. Trimmomatic: a flexible trimmer for
870 Illumina sequence data. Bioinformatics 30:2114-20.
871 84. Prjibelski A, Antipov D, Meleshko D, Lapidus A, Korobeynikov A. 2020. Using
872 SPAdes De Novo Assembler. Curr Protoc Bioinformatics 70:e102.

85. Cherny KE, Ozer EA, Kochan TJ, Kociolek LK. 2020. Complete Genome Sequence of *Clostridium innocuum* Strain ATCC 14501. Microbiol Resour Announc 9.
86. Cherny KE, Ozer EA, Kochan TJ, Johnson S, Kociolek LK. 2020. Complete Genome Sequence of *Clostridium innocuum* Strain LC-LUMC-CI-001, Isolated from a Patient with Recurrent Antibiotic-Associated Diarrhea. Microbiol Resour Announc 9.
87. Wick RR, Judd LM, Holt KE. 2019. Performance of neural network basecalling tools for Oxford Nanopore sequencing. Genome Biol 20:129.
88. Tatusova T, DiCuccio M, Badretdin A, Chetvernin V, Nawrocki EP, Zaslavsky L, Lomsadze A, Pruitt KD, Borodovsky M, Ostell J. 2016. NCBI prokaryotic genome annotation pipeline. Nucleic Acids Res 44:6614-24.
89. Hadano Y. 2013. String test. BMJ Case Rep 2013.
90. Price MN, Dehal PS, Arkin AP. 2010. FastTree 2--approximately maximum-likelihood trees for large alignments. PLoS One 5:e9490.
91. Letunic I, Bork P. 2021. Interactive Tree Of Life (iTOL) v5: an online tool for phylogenetic tree display and annotation. Nucleic Acids Res 49:W293-W296.
92. Wick RR, Heinz E, Holt KE, Wyres KL. 2018. Kaptive Web: User-Friendly Capsule and Lipopolysaccharide Serotype Prediction for *Klebsiella* Genomes. J Clin Microbiol 56.
93. Alikhan NF, Petty NK, Ben Zakour NL, Beatson SA. 2011. BLAST Ring Image Generator (BRIG): simple prokaryote genome comparisons. BMC Genomics 12:402.
94. Carattoli A, Zankari E, Garcia-Fernandez A, Voldby Larsen M, Lund O, Villa L, Moller Aarestrup F, Hasman H. 2014. In silico detection and typing of plasmids using PlasmidFinder and plasmid multilocus sequence typing. Antimicrob Agents Chemother 58:3895-903.
95. Ritz C, Baty F, Streibig JC, Gerhard D. 2015. Dose-Response Analysis Using R. PLoS One 10:e0146021.

Figure Legends

Figure 1. Virulence plasmids associated with hypervirulence in *Klebsiella pneumoniae*. PAL-1 and PAL-2 contents and organization are depicted for pK2044,

KP52.145pII, pTK421_2, and ICEKp1 **(A)**. Genomic elements and plasmid architecture are depicted for pK2044 **(B)**, KP52.145pII **(C)** and pTK421 **(D)**. (Drawings not to scale.)

Figure 2. Core genome phylogenetic tree of 104 *Klebsiella pneumoniae* bloodstream isolates. Maximum likelihood phylogenetic tree generated from core genome SNP loci in 104 *K. pneumoniae* bloodstream isolates. Sequence types, the presence of virulence factors, and antibiotic resistances are indicated. *ybt* = yersiniabactin biosynthesis loci, *clb* = colibactin biosynthesis loci, *rmpADC* = mucoid regulator operon, *rmpA2* = regulator of mucoid phenotype 2, *iuc* = aerobactin biosynthesis genes, *iro* = salmochelin biosynthesis genes, Amp = ampicillin, TMP/SMX = trimethoprim-sulfamethoxazole. Strains were considered Hypermucoviscous if they were positive by string test. The complete genome of NTUH-K2044 is used as the reference genome.

Figure 3. The bloodstream isolates KPN115 and KPN8 harbor pK2044-like plasmids. pKPN115_1 and pKPN8_1 sequences were aligned to pK2044 using blast ring image generator (BRIG). A sequence identity threshold of 85% was used. Aerobactin biosynthesis genes are indicated with green arrows, salmochelin with orange arrows, *rmpA* with a blue arrow, and *rmpA2* with a red arrow.

Figure 4. The bloodstream isolates KPN49 and KPN165 harbor KP52.145pII-like plasmids. A. The indicated plasmids sequences were aligned to KP52.145pII using blast ring image generator (BRIG). **B.** The indicated plasmids sequences were aligned to pKPN49_1 using blast ring image generator (BRIG). A sequence identity threshold of

85% was used. Aerobactin biosynthesis genes are indicated with green arrows, salmochelin with orange arrows, and *rmpA* with a blue arrow.

Figure 5. The bloodstream isolate KPN23 harbors a unique plasmid containing aerobactin biosynthesis genes. The indicated plasmids were aligned to that of KPCTRSRTH01_p2. **(A)** or pK2044, KP52.145pII, and pTK421_2 **(B)** were aligned with pKpN23_1 using blast ring image generator (BRIG). A sequence identity threshold of 85% was used. Aerobactin biosynthesis genes are indicated with green arrows. Aerobactin biosynthesis genes are indicated with green arrows.

Figure 6. NMH Isolates containing hvKp pathogenicity loci were extremely virulent in a murine model of pneumonia. C57BL/6 mice were infected by nasal aspiration with the indicated doses of hvKP5 **(A)**, TK421 **(B)**, KPN8 **(C)**, KPN23 **(D)**, KPN49 **(E)**, and KPN80 **(F)**. Genotypes, phenotypes, and calculated LD50s are listed in Table 1.

Tables.

Table 1. Genomic Characteristics of bloodstream isolates containing hvKp pathogenicity loci

Strain	ST	K-Locus	*iuc*	*iro*	hmv*	*rmpA/2*	Plasmid	Virulence Plasmid Replicon	Other Plasmid Replicon	LOGLD50
KPN8	ST23	KL1	*iuc 1*	*iro 1*	+	*rmpA, rmpA2*	pKPN8_1	repB, IncHI1B(pNDM-MAR)		2.22
KPN23	ST881	KL2	*iuc 3*	-	-	-	pKPN23_1	IncFIB(K), IncFII(pKP91)	ColRNAI	6.07
KPN49	ST66	KL2	*iuc 2*	*iro 2*	+	*rmpA*	pKPN49_1	IncFIB(K)	IncFIA(HI1)	1.51
KPN115	ST23	KL1	*iuc 1*	*iro 1*	+	*rmpA, rmpA2*	pK2044	repB, IncHI1B(pNDM-MAR)	IncFIB(pKPHS1)	NT*
KPN165	ST380	KL2	*iuc 2*	*iro 2*	+	*rmpA*	pKPN165_1	IncFIB(K)		NT*
KPN80	ST29	KL30	-	-	+	-	NT			8.06
TK421	ST34	KL20	iuc 2	iro 2	+	rmpA	pTK421_2	repB, IncR	IncFII(pKP91), IncFIA(HI1)	4.52
hvKP5	ST23	KL1	*iuc 1*	*iro 1*	+	*rmpA, rmpA2*	pK2044	repB, IncHI1B(pNDM-MAR)	IncFIB(pKPHS1)	1.98

*hmv: hypermucoviscosity
*NT: Not Tested

Table 2. Virulence factors identified in NMH bloodstream isolates

Isolates n = 104	Positive n(%)
iroB	4 (3.8)
iucA	5 (4.2)
rmpA	4 (3.8)
rmpA2	2 (1.9)
ybt	39 (37.5)
clb	12 (11.5)
iroB/iucA/rmpA	4 (4.2)
String Test	10 (9.6)
Centrifugation Test	18 (17.3)
Tellurite Resistance	5 (4.8)

Table 3. Clinical Characteristics of bloodstream isolates containing hvKp° pathogenicity loci

Strain	Age (Years)	Type of Infection	Community-Acquired Infection	Medical Comorbidities
KPN8	67	Bloodstream only	No	Type II Diabetes, Myocardial Infarction, Peripheral Vascular Disease
KPN23	50	Bloodstream only	No	Pancreatic Adenocarcinoma
KPN49	53	Pneumonia/lung abscess	Yes	HIV
KPN115	73	Hepatic Abscess	Yes	Type II Diabetes, Colon Adenocarcinoma
KPN165	50	Hepatic Abscess	Yes	Cholangiocarcinoma
KPN80	68	Pneumonia	Yes	Cirrhosis
TK421	65	Hepatic Abscess	Yes	Type II Diabetes, Pancreatic Adenocarcinoma

Key
° Hypervirulent *Klebsiella pneumoniae*

Supplemental Figure Legends

Figure S1. Population structure of *Klebsiella* spp. bloodstream isolates. Maximum likelihood phylogenetic tree generated from core genome SNP loci in 140 *Klebsiella* spp.

bloodstream isolates. The tree has a truncated outlier branch for *Klebsiella oxytoca* (yellow). The scale bars represent genetic distances.

Figure S2. NMH *K. pneumoniae* bloodstream isolates are highly diverse in ST, KL, and O antigen. Numbers of genomes with each corresponding ST **(A)**, KL **(B)**, or O-antigen type **(C)** were determined using *Kleborate* and *Kaptive*.

Figure S3. Antimicrobial resistance phenotypes of *K. pneumoniae* bloodstream isolates. The percentage of isolates resistant (solid bars) or intermediately susceptible (cross-hatched bars) to the indicated antibiotics are shown. Antibiotic classes are grouped by color.

Figure S4. Beta-lactam resistant isolates contain a variety of extended-spectrum beta-lactamase or carbapenamase genes. Numbers of genomes containing the indicated beta-lactamase genes present in isolates resistant to ceftriaxone **(A)**, meropenem **(B)**, amp/sulbactam **(C)**, aztreonam **(D)**, cefazolin **(E)**, or cefepime **(F)** are plotted. "-" indicates strains without an extended-spectrum beta-lactamase.

Figure S5. pKPN49_2, pKPN165_1, pTK421_2, and pKPN23_1 have little similarity to pK2044. DNA sequences of these plasmids were aligned to pK2044 using blast ring image generator (BRIG). A sequence identity threshold of 85% was used. Aerobactin

biosynthesis genes are indicated with green arrows, salmochelin with orange arrows, *rmpA* with a blue arrow, and *rmpA2* with a red arrow.

Figure S6. Core genome phylogenetic tree of United States hypervirulent *Klebsiella pneumoniae* isolates. A maximum likelihood phylogenetic tree was generated from core genome SNP loci in hvKP isolates from United States hospitals and select global reference isolates. Sequence types are indicated. The presence of virulence factors is listed next to each isolate: *ybt* = yersiniabactin biosynthesis loci, *clb* = colibactin biosynthesis loci, *rmpADC* = mucoid regulator operon, *rmpA2* = regulator of mucoid phenotype 2, *iuc* = aerobactin biosynthesis genes, *iro* = salmochelin biosynthesis genes. The scale bars represent genetic distances. KPPR1, KP52.145, SB5881, K180005, NCTC9494, NTUH-K2044, RJF999, and ED2 are global isolates used as a reference.

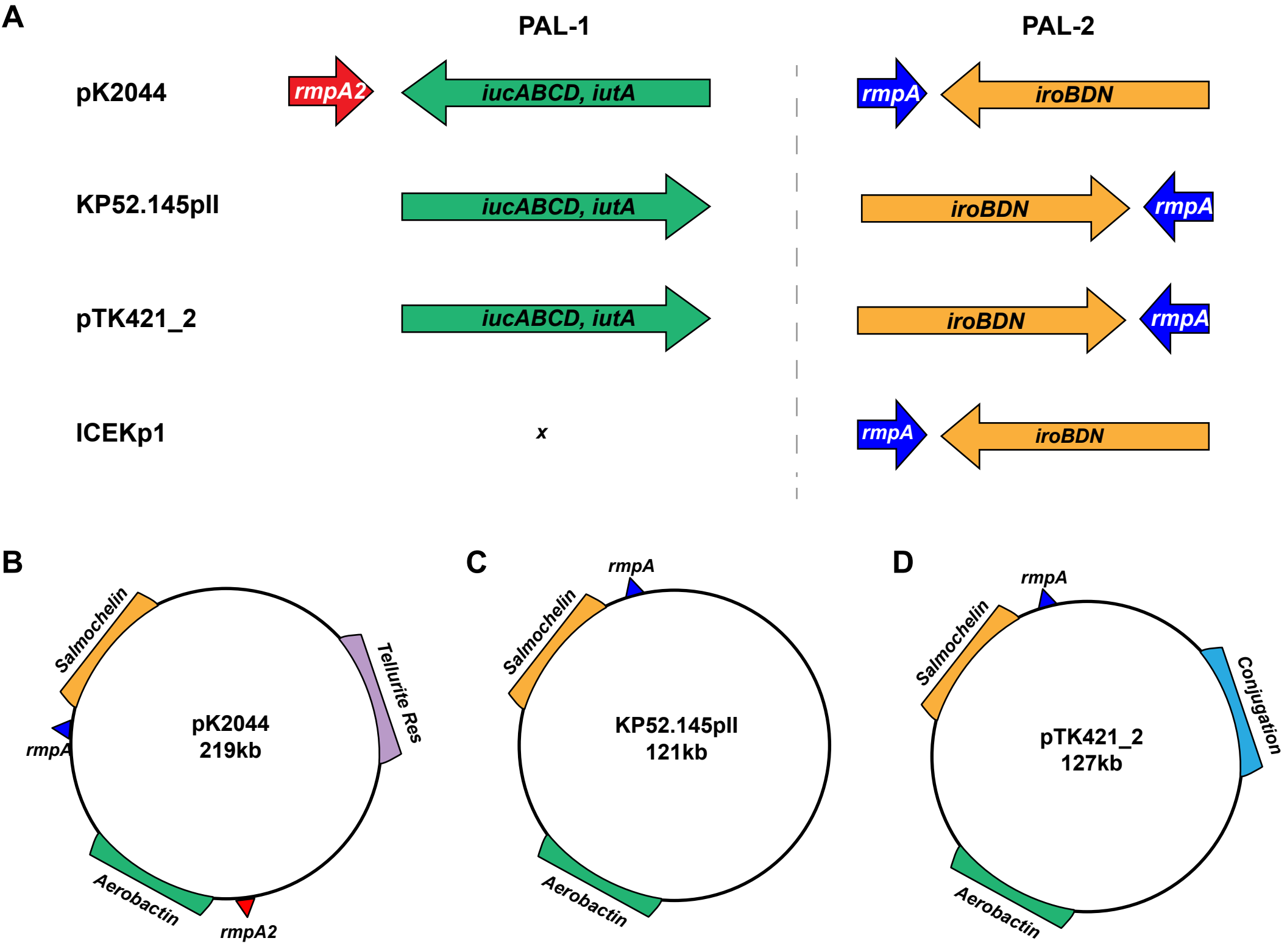
A
PAL-1
PAL-2
pK2044
rmpA2
iucABCD, iutA
rmpA
iroBDN
KP52.145pII
iucABCD, iutA
iroBDN
rmpA
pTK421_2
iucABCD, iutA
iroBDN
rmpA
ICEKp1
x
rmpA
iroBDN
B
Salmochelin
Tellurite Res
pK2044
219kb
rmpA
Aerobactin
rmpA2
C
rmpA
Salmochelin
KP52.145pII
121kb
Aerobactin
D
rmpA
Salmochelin
Conjugation
pTK421_2
127kb
Aerobactin

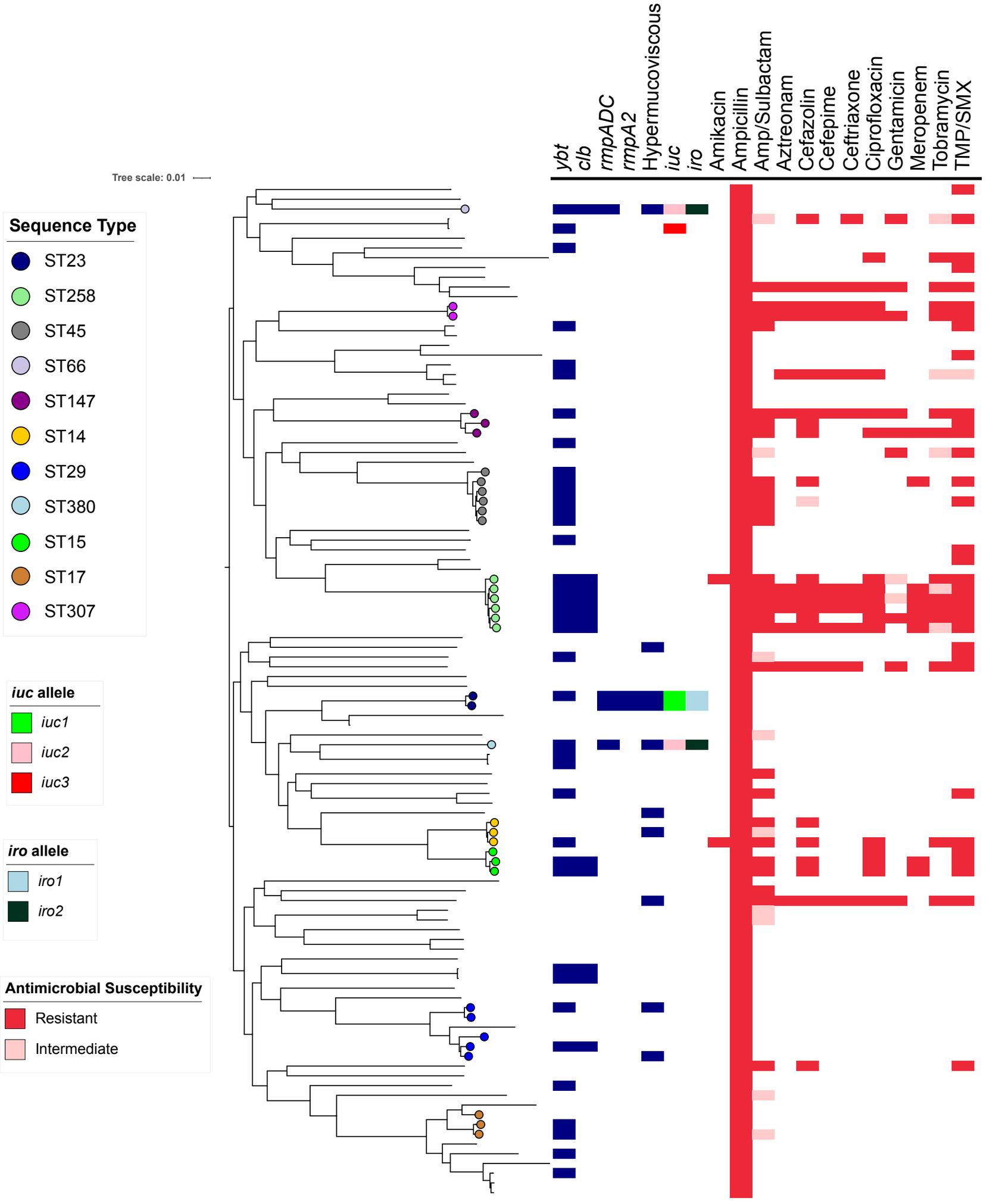
Tree scale: 0.01
Sequence Type
ST23
ST258
ST45
ST66
ST147
ST14
ST29
ST380
ST15
ST17
ST307
iuc allele
iuc1
iuc2
iuc3
iro allele
iro1
iro2
Antimicrobial Susceptibility
Resistant
Intermediate
ybt
clb
rmpADC
rmpA2
Hypermucoviscous
iuc
iro
Amikacin
Ampicillin
Amp/Sulbactam
Aztreonam
Cefazolin
Cefepime
Ceftriaxone
Ciprofloxacin
Gentamicin
Meropenem
Tobramycin
TMP/SMX

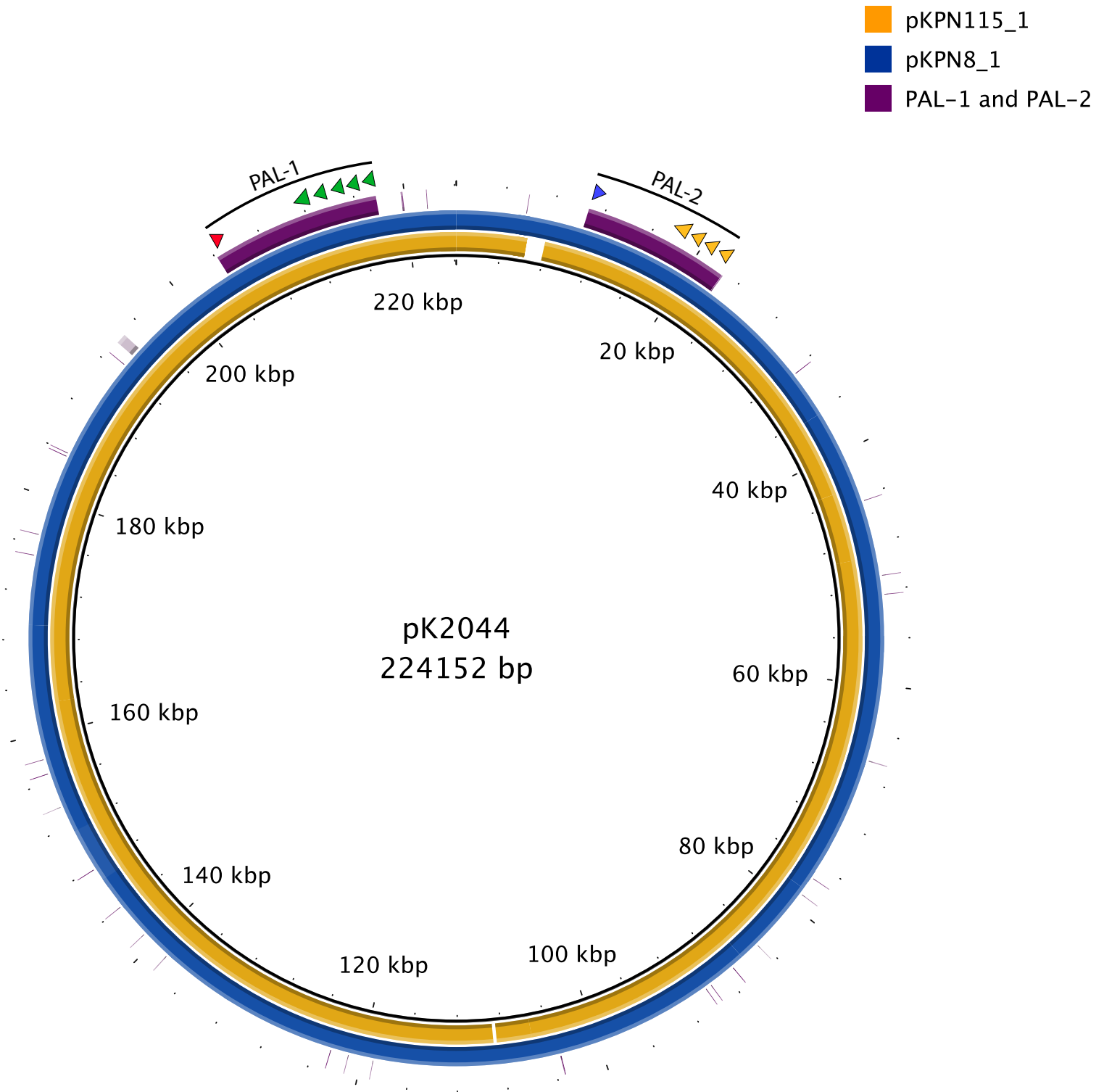
pKPN115_1
pKPN8_1
PAL-1 and PAL-2
PAL-1
PAL-2
220 kbp
20 kbp
40 kbp
60 kbp
80 kbp
100 kbp
120 kbp
140 kbp
160 kbp
180 kbp
200 kbp
pK2044
224152 bp

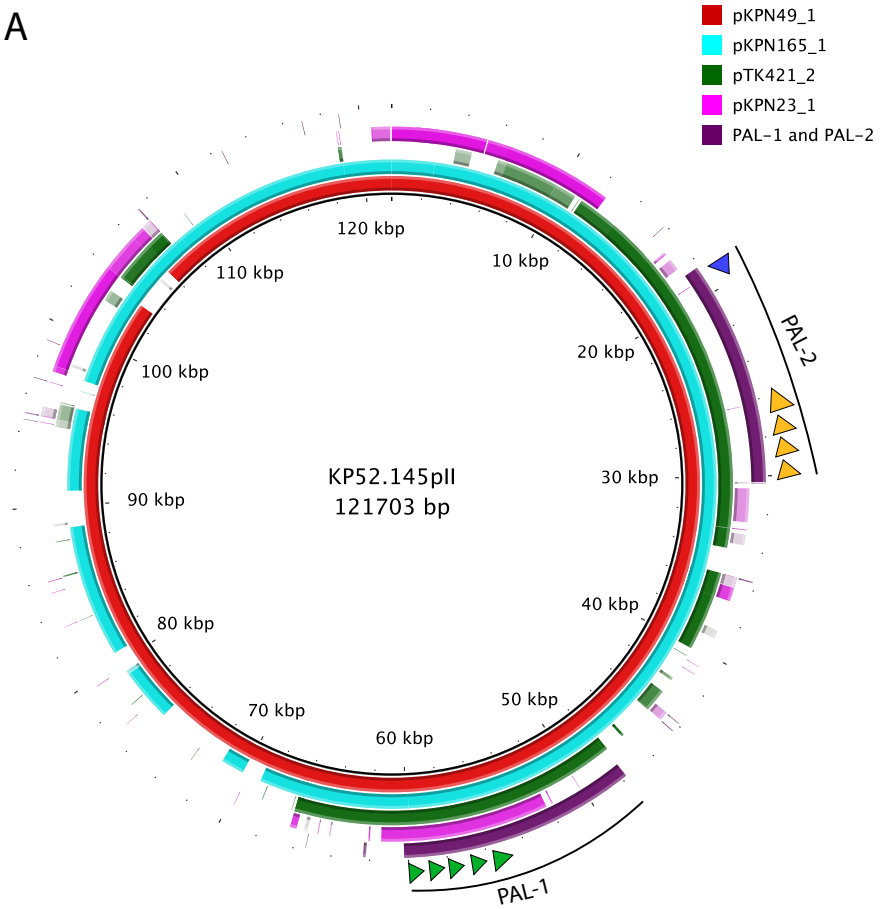
A
pKPN49_1
pKPN165_1
pTK421_2
pKPN23_1
PAL-1 and PAL-2
KP52.145pII
121703 bp
10 kbp
20 kbp
30 kbp
40 kbp
50 kbp
60 kbp
70 kbp
80 kbp
90 kbp
100 kbp
110 kbp
120 kbp
PAL-1
PAL-2

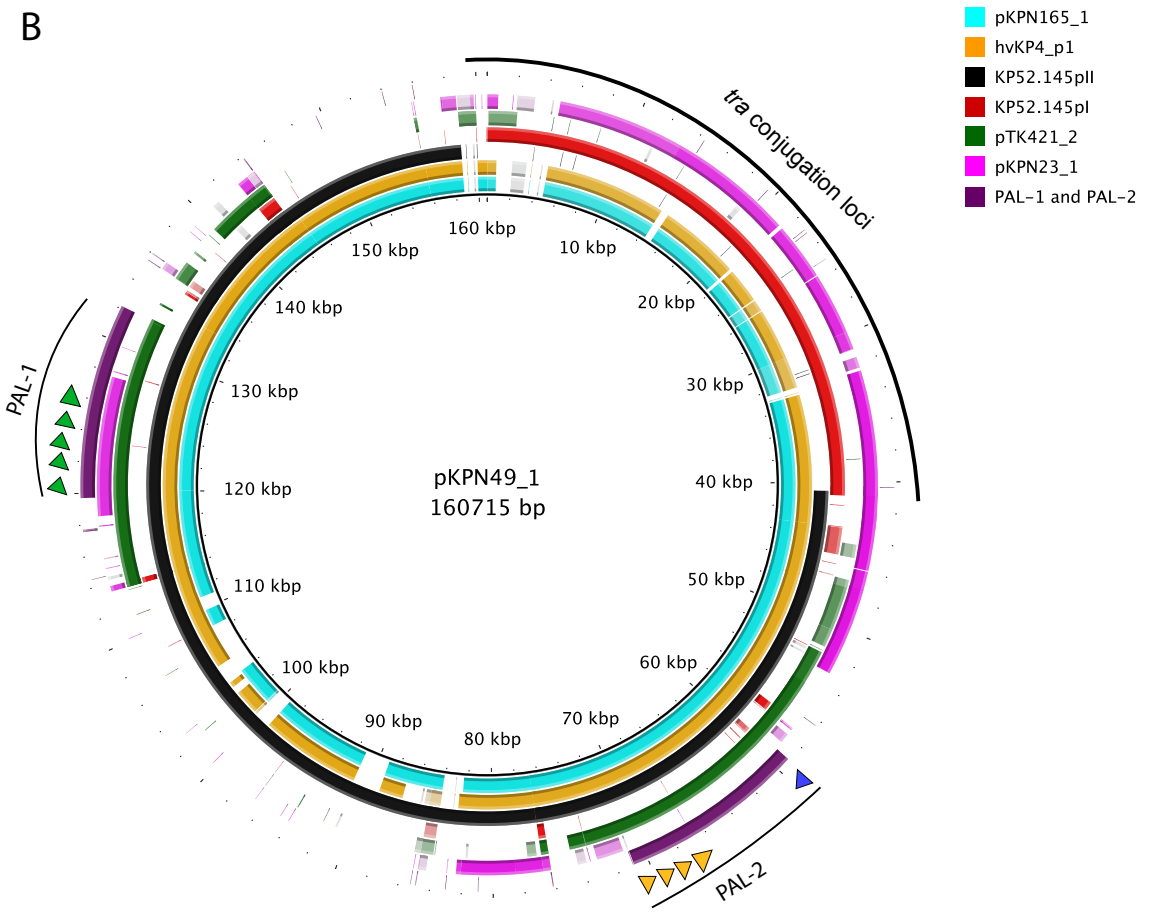
B
pKPN165_1
hvKP4_p1
KP52.145pII
KP52.145pI
pTK421_2
pKPN23_1
PAL-1 and PAL-2
tra conjugation loci
pKPN49_1
160715 bp
10 kbp
20 kbp
30 kbp
40 kbp
50 kbp
60 kbp
70 kbp
80 kbp
90 kbp
100 kbp
110 kbp
120 kbp
130 kbp
140 kbp
150 kbp
160 kbp
PAL-1
PAL-2

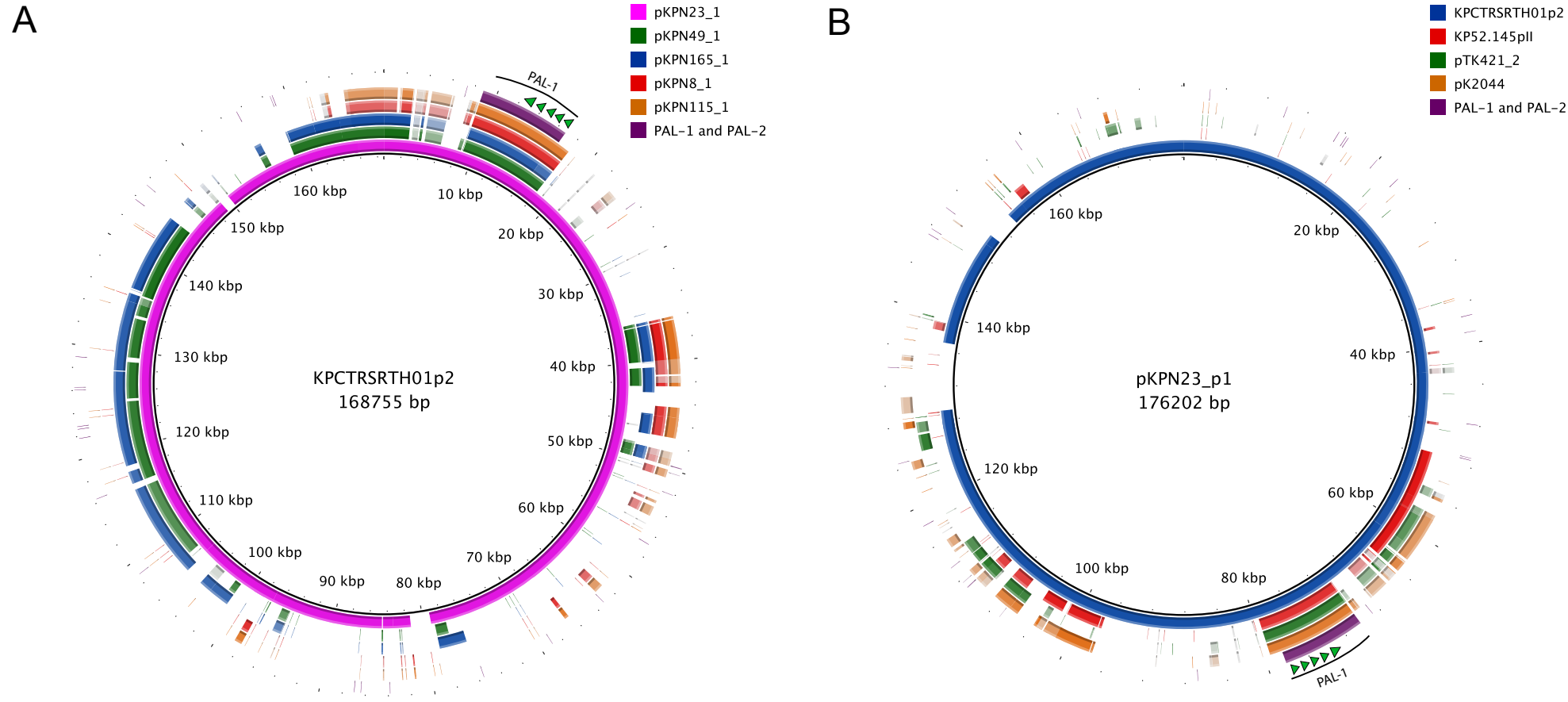
A
pKPN23_1
pKPN49_1
pKPN165_1
pKPN8_1
pKPN115_1
PAL-1 and PAL-2
PAL-1
KPCTRSRTH01p2
168755 bp
10 kbp
20 kbp
30 kbp
40 kbp
50 kbp
60 kbp
70 kbp
80 kbp
90 kbp
100 kbp
110 kbp
120 kbp
130 kbp
140 kbp
150 kbp
160 kbp
B
KPCTRSRTH01p2
KP52.145pII
pTK421_2
pK2044
PAL-1 and PAL-2
PAL-1
pKPN23_p1
176202 bp
20 kbp
40 kbp
60 kbp
80 kbp
100 kbp
120 kbp
140 kbp
160 kbp

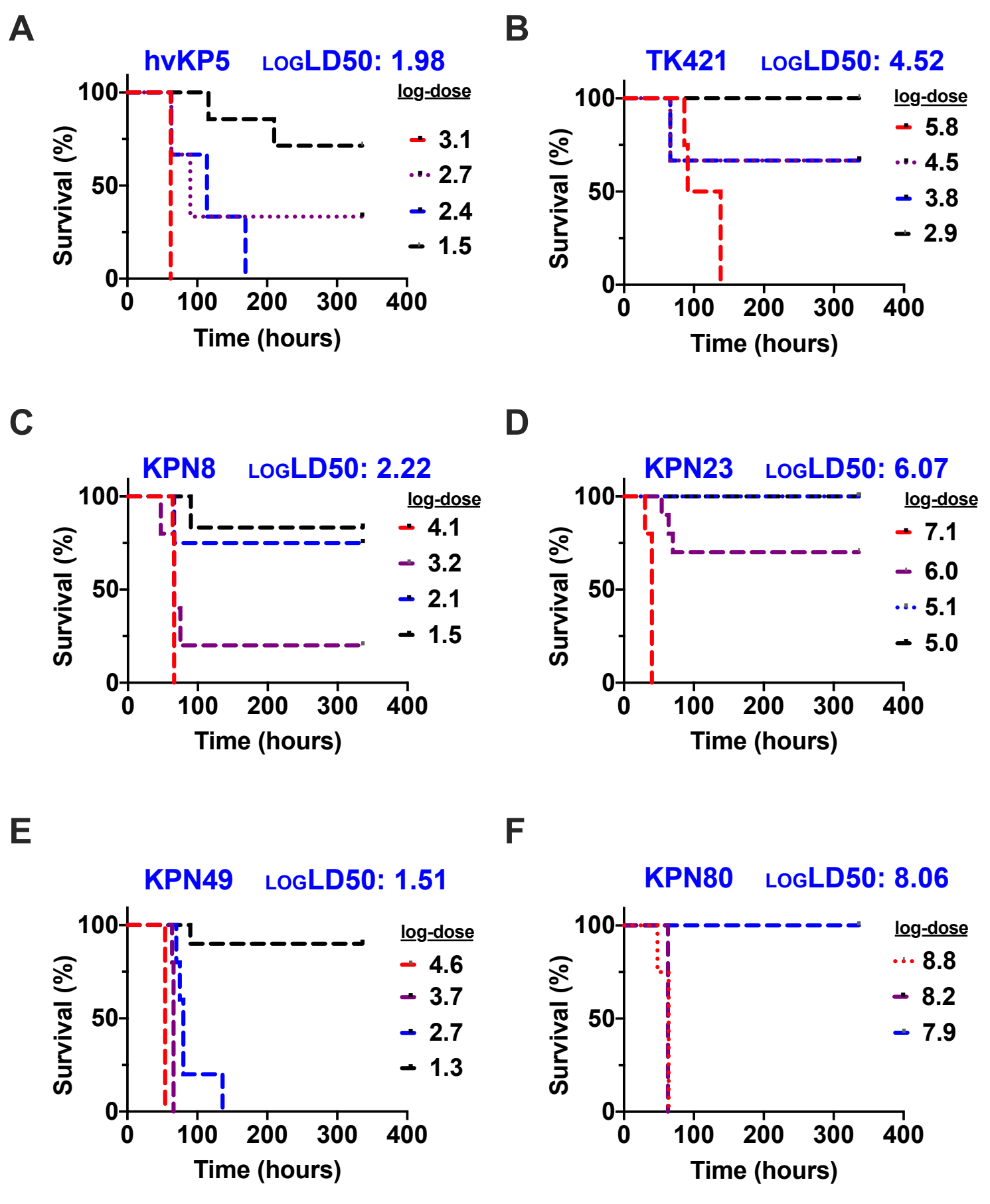
A
hvKP5 LOGLD50: 1.98
log-dose
3.1
2.7
2.4
1.5
Survival (%)
Time (hours)
B
TK421 LOGLD50: 4.52
log-dose
5.8
4.5
3.8
2.9
Survival (%)
Time (hours)
C
KPN8 LOGLD50: 2.22
log-dose
4.1
3.2
2.1
1.5
Survival (%)
Time (hours)
D
KPN23 LOGLD50: 6.07
log-dose
7.1
6.0
5.1
5.0
Survival (%)
Time (hours)
E
KPN49 LOGLD50: 1.51
log-dose
4.6
3.7
2.7
1.3
Survival (%)
Time (hours)
F
KPN80 LOGLD50: 8.06
log-dose
8.8
8.2
7.9
Survival (%)
Time (hours)